

Aggregation control of Ru and Ir nanoparticles by tunable aryl alkyl imidazolium ionic liquids

Laura Schmolke,^a Swantje Lerch,^b Mark Bülow,^c Marvin Siebels,^a Alexa Schmitz,^a Jörg Thomas,^d Gerhard Dehm,^d Christoph Held,^c Thomas Strassner,^{*b} and Christoph Janiak,^{*a}

Address: ^a Institut für Anorganische Chemie und Strukturchemie, Heinrich-Heine-Universität

Düsseldorf, 40204 Düsseldorf, Germany. Fax: +49-211-81-12287; Tel: +49-211-81-12286.

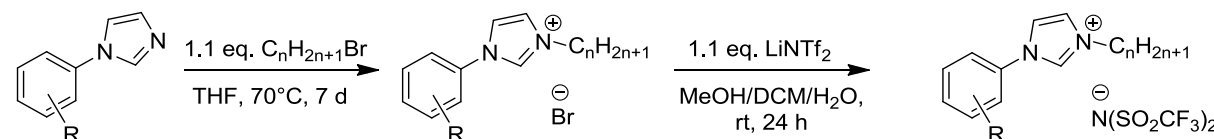
Email: janiak@uni-duesseldorf.de

^b Professur für Physikalische Organische Chemie, Technische Universität Dresden, 01062 Dresden

^c Laboratory of Thermodynamics, Technische Universität Dortmund, Emil-Figge-Str 70, 44227 Dortmund, Germany. Email: Christoph.Held@tu-dortmund.de

^d Department Structure and Nano- / Micromechanics of Materials, Max-Planck-Institut für Eisenforschung GmbH, 40237 Düsseldorf, Germany.

1 Synthesis of TAAILs



Scheme S1 General synthesis of TAAILs with different aryl substitutions and chain lengths.

The synthesis of the tunable aryl alkyl ionic liquids (TAAILs) was a two step synthesis (Scheme S1). The first step was the alkylation of the aryl imidazoles by bromoalkanes to build the IL-cations. In the second step the anion (bromide) was exchanged with LiNTf₂.

NMR spectra were recorded on a Bruker-AC-300P NMR spectrometer operating at 300.13 MHz for ¹H, 75.48 MHz for ¹³C and 282.4 MHz for ¹⁹F. CDCl₃ was used as solvent. Chemical shifts were reported relative to Si(CH₃)₄ (0 ppm) for ¹H- and ¹³C-NMR. Elemental analysis was performed on a EUROVEKTOR Hekatech EA3000. Dichloromethane was distilled prior to use. All other chemicals were used as received without further purification.

1.1 Synthesis of Bromide-ILs

General procedure: In a round-bottom flask equipped with a pressure release valve 1 equiv. of aryl imidazole is dissolved in THF. 1.1 equiv. of the corresponding bromoalkane are added and the reaction mixture is heated to 70°C for 7 days. The solvent is removed under reduced pressure. The crude product is washed with ethyl acetate and pentane.

1-(2-methylphenyl)-3-pentyl-1H-imidazolium bromide

The product was obtained as a highly viscous oil (219 g, 693 mmol, 100 %).

¹H NMR (CDCl₃, 300.13 MHz): δ 10.64 (s, 1 H, NCHN), 7.64 - 7.71 (s, 1 H, NCHCHN), 7.30 - 7.50 (m, 5 H, NCHCHN, H_{ar}), 4.69 (t, J=7.46 Hz, 2 H, NCH₂), 2.30 (s, 3 H, CH₃), 1.94 - 2.05 (m, 2 H, CH₂), 1.27 - 1.45 (m, 4 H, CH₂), 0.84 - 0.95 (m, 3 H, CH₃). ¹³C NMR (CDCl₃, 125.75 MHz): δ 137.5 (NCHN), 133.7 (NC_{ar}), 133.2 (CH₃C_{ar}), 132.0 (C_{ar}H), 131.0 (C_{ar}H), 127.7 (C_{ar}H), 126.2 (C_{ar}H), 123.1 (NCHCHN), 122.5 (NCHCHN), 50.4 (NCH₂), 30.1 (CH₂), 28.2 (CH₂), 22.1 (CH₂), 17.9 (CH_{3,ar}), 13.8 (CH₃). Elemental analysis: calc. for C₁₅H₂₁BrN₂: C: 58.26%, H: 6.84%, N: 9.06%, found: C: 57.91%, H: 6.88%, N: 9.28%.

1-(4-methoxyphenyl)-3-pentyl-1H-imidazolium bromide

The product was obtained as a light brown solid (26.5 g, 81 mmol, 95 %).

¹H NMR (CDCl₃, 300.13 MHz): δ 10.98 (s, 1 H, NCHN), 7.72 (d, J=9.06 Hz 2 H, H_{ar}), 7.64 (m, 1 H, NCHCHN), 7.53 (m, 1 H, NCHCHN), 7.03 (d, J=8.88 Hz, 2 H, H_{ar}), 4.56 (t, J=7.46 Hz, 2 H, NCH₂), 3.83 (s, 3 H, OCH₃), 1.92 - 2.04 (m, 2 H, CH₂), 1.31 - 1.42 (m, 4 H, CH₂), 0.83 - 0.95 (m, 3 H, CH₃). ¹³C NMR (CDCl₃, 75.48 MHz): 160.7 (NC_{ar}), 135.9 (NCHN), 127.4 (OC_{ar}), 123.3 (C_{ar}H), 122.4 (NCHCHN), 120.7 (NCHCHN), 115.5 (C_{ar}H), 55.7 (OCH₃), 50.4 (NCH₂), 30.0 (CH₂), 28.2 (CH₂), 22.1 (CH₂), 13.8 (CH₃). Elemental analysis: calc. for C₁₅H₂₁BrN₂O: C: 55.39%, H: 6.51%, N: 8.61%, found: C: 55.03%, H: 6.60%, N: 8.75%.

1-(4-methoxyphenyl)-3-octyl-1H-imidazolium bromide

The product was obtained as an ivory solid (24.0 g, 65 mmol, 76 %).

¹H NMR (CDCl₃, 300.13 MHz): δ 11.23 (s, 1 H, NCHN), 7.72 (d, J=8.88 Hz, 2 H, H_{ar}), 7.52 (s, 1 H, NCHCHN), 7.39 (s, 1 H, NCHCHN), 7.05 (d, J=9.06 Hz, 2 H, H_{ar}), 4.57 (t, J=7.46 Hz, 2 H, NCH₂), 3.85 (s, 3 H, OCH₃), 1.93 - 2.06 (m, 2 H, CH₂), 1.36 - 1.25 (m, 10 H, CH₂), 0.82 - 0.89 (m, 3 H, CH₃). ¹³C NMR (CDCl₃, 75.48 MHz): 160.6 (NC_{ar}), 135.7 (NCHN), 127.4 (OC_{ar}), 123.2 (C_{ar}H), 122.6 (NCHCHN), 120.8 (NCHCHN), 115.4 (C_{ar}H), 55.7 (OCH₃), 50.4 (NCH₂), 31.6 (CH₂), 28.9 (CH₂), 28.9 (CH₂), 26.2 (CH₂), 22.5 (CH₂), 14.0 (CH₃). Elemental analysis: calc. for C₁₈H₂₇BrN₂O: C: 58.86%, H: 7.41%, N: 7.63%, found: C: 59.15%, H: 7.79%, N: 8.15%.

1-(2,4-dimethylphenyl)-3-pentyl-1H-imidazolium bromide

The product was obtained as a yellow solid (225 g, 696 mmol, 100 %).

¹H NMR (CDCl₃, 300.13 MHz): δ 10.61 (t, J=1.51 Hz, 1 H, NCHN), 7.61 (t, J=1.70 Hz, 1 H, NCHCHN), 7.30 (t, J=1.70 Hz, 1 H, NCHCHN), 7.27 (s, 1 H, H_{ar}), 7.08 - 7.21 (m, 2 H, H_{ar}), 4.69 (t, J=7.37 Hz, 2 H, NCH₂), 2.38 (s, 3 H, CH_{3,ar}), 2.25 (s, 3 H, CH_{3,ar}), 1.91 - 2.07 (m, 2 H, CH₂), 1.30 - 1.47 (m, 4 H, CH₂), 0.85 - 0.98 (m, 3 H, CH₃). ¹³C NMR (CDCl₃, 75.48 MHz): 141.5 (NC_{ar}), 137.9 (NCHN), 132.7 (CH₃C_{ar}), 132.6 (C_{ar}H), 131.2 (CH₃C_{ar}), 128.3 (C_{ar}H), 125.9 (C_{ar}H), 123.0 (NCHCHN), 122.0 (NCHCHN), 50.4 (NCH₂), 30.1 (CH₂), 28.2 (CH₂), 22.1 (CH₂), 21.1 (CH_{3,ar}), 17.8 (CH_{3,ar}), 13.8 (CH₃). Elemental analysis: calc. for C₁₆H₂₃BrN₂: C: 59.45%, H: 7.17%, N: 8.67%, found: C: 59.41%, H: 7.55%, N: 8.58%.

1-(2,4-dimethylphenyl)-3-nonyl-1H-imidazolium bromide

The product was obtained as a yellow solid (346 g, 912 mmol, 100 %).

¹H NMR (CDCl₃, 300.13 MHz): δ 10.46 (s, 1 H, NCHN), 7.52 - 7.63 (m, 1 H, NCHCHN), 7.27 - 7.36 (m, 2 H, H_{ar}), 7.10 - 7.22 (m, 2 H, H_{ar}, NCHCHN), 4.66 (t, J=7.37 Hz, 2 H, NCH₂), 2.39 (s, 3 H, CH_{3,ar}), 2.25 (s, 3 H, CH_{3,ar}), 1.91 - 2.08 (m, 2 H, CH₂), 1.36 - 1.13 (m, 12 H, CH₂), 0.87 (t, J=6.42 Hz, 3 H, CH₃). ¹³C NMR (CDCl₃, 75.48 MHz): 141.5 (NC_{ar}), 137.7 (NCHN), 132.8 (CH₃C_{ar}), 132.6 (C_{ar}H), 131.3 (CH₃C_{ar}), 128.3 (C_{ar}H), 125.9 (C_{ar}H), 123.1 (NCHCHN), 122.1 (NCHCHN), 50.5 (NCH₂), 31.7 (CH₂), 30.4 (CH₂), 29.3 (CH₂), 29.1 (CH₂), 29.0 (CH₂), 26.2 (CH₂), 22.6 (CH₂), 21.1 (CH_{3,ar}), 17.8 (CH_{3,ar}), 14.0 (CH₃). Elemental analysis: calc. for C₂₀H₃₁BrN₂: C: 62.32%, H: 8.24%, N: 7.09%, found: C: 62.19%, H: 8.59%, N: 7.11%.

1.2 Synthesis of Bis(trifluoromethylsulfonyl)imide-ILs

General procedure: In a round bottom flask, the corresponding bromide salt¹⁻³ (1 equiv.) was dissolved in methanol. 1.1 equiv. of LiNTf₂ (70% aq. solution) and additional water were added to the reaction mixture. The two phase system was diluted with dichloromethane and stirred at room temperature for 24 h. The organic phase was extracted two times with DCM, washed with water twice and dried over magnesium sulphate. The solvent was removed *in vacuo* to yield the liquid product. Characterization was done by ¹H-NMR, ¹³C-NMR, ¹⁹F-NMR and elemental analysis.

1-(2-methylphenyl)-3-butyl-1H-imidazolium bis(trifluoromethylsulfonyl)imide (**2a**)

The product was obtained as a yellow oil (31.9 g, 64.5 mmol, 95 %).

¹H NMR (CDCl₃, 300.13 MHz): δ 8.86 (s, 1 H, NCHN), 7.45 - 7.57 (m, 2 H, NCHCHN + H_{ar}), 7.32 - 7.45 (m, 4 H, NCHCHN + H_{ar}), 4.36 (t, J=7.46 Hz, 2 H, NCH₂), 2.21 (s, 3 H, CH_{3,ar}), 1.94 (quin, J=7.60 Hz, 2 H, CH₂), 1.34 - 1.50 (m, 2 H, CH₂), 0.99 (t, J=7.37 Hz, 3 H, CH₃). ¹³C NMR (CDCl₃, 75.48 MHz): δ 136.0 (NCHN), 133.4 (NC_{ar}), 133.2 (C_{ar}CH₃), 132.0 (C_{ar}H), 131.4 (C_{ar}H), 127.8 (C_{ar}H), 126.3 (C_{ar}H), 123.7 (NCHCHN), 122.6 (NCHCHN), 119.7 (q, J=321.3 Hz, CF₃), 50.4 (CH₂), 31.9 (CH₂), 19.4 (CH₂), 17.2 (CH_{3,ar}), 13.3 (CH₃). ¹⁹F NMR (CDCl₃, 282.4 MHz): δ -79.7. Calc. for C₁₆H₁₉F₆N₃O₄S₂: C: 38.79%, H: 3.87%, N: 8.48%, S: 12.94%, Found: C: 38.40%, H: 3.94%, N: 8.78%, S: 12.60%.

1-(2-methylphenyl)-3-pentyl-1H-imidazolium bis(trifluoromethylsulfonyl)imide (2b)

The product was obtained as a light green oil (278 g, 546 mmol, 88 %).

¹H NMR (CDCl₃, 300.13 MHz): δ 8.87 (br. s., 1 H, NCHN), 7.45 - 7.56 (m, 2 H, NCHCHN + H_{ar}) 7.32 - 7.45 (m, 4 H, NCHCHN + H_{ar}), 4.36 (t, J=7.37 Hz, 2 H, NCH₂), 2.22 (s, 3 H, CH_{3,ar}), 1.91 - 2.02 (m, 2 H, CH₂), 1.31 - 1.45 (m, 4 H, CH₂), 0.89 - 0.96 (m, 3 H, CH₃). ¹³C NMR (CDCl₃, 75.48 MHz): δ 136.0 (NCHN), 133.4 (NC_{ar}), 133.2 (C_{ar}CH₃), 132.0 (C_{ar}H), 131.4 (C_{ar}H), 127.8 (C_{ar}H), 126.2 (C_{ar}H), 123.8 (NCHCHN), 122.6 (NCHCHN), 119.7 (q, J=321.3 Hz, CF₃), 50.6 (CH₂), 29.7 (CH₂), 28.1 (CH₂), 21.9 (CH₂), 17.2 (CH_{3,ar}), 13.7 (CH₃). ¹⁹F NMR (CDCl₃, 282.4 MHz): δ -79.6. Calc. for C₁₇H₂₁F₆N₃O₄S₂: C: 40.08%, H: 4.15%, N: 8.25%, S: 12.59%; Found: C: 39.71%, H: 4.15%, N: 8.56%, S: 12.51%.

1-(2-methylphenyl)-3-nonyl-1H-imidazolium bis(trifluoromethylsulfonyl)imide (2d)

The product was obtained as a brown liquid (557 g, 980 mmol, 86 %).

¹H NMR (CDCl₃, 300.13 MHz): δ 8.86 (s, 1 H, NCHN), 7.46 - 7.55 (m, 2 H, H_{ar}), 7.33 - 7.44 (m, 4 H, H_{ar}, NCHCHN), 4.35 (t, J=7.55 Hz, 2 H, NCH₂), 2.22 (s, 3 H, CH_{3(ar)}), 1.89 - 2.01 (m, 2 H, CH₂), 1.24 - 1.36 (m, 12 H CH₂), 0.87 (4, J=6.80 Hz, 3 H, CH₃). ¹³C NMR (CDCl₃, 75.475 MHz): δ 136.0 (NCHN), 133.5 (N-C_{ar}), 133.2 (C_{ar}), 132.0 (C_{ar}H), 131.4 (C_{ar}H), 127.9 (C_{ar}H), 126.3 (C_{ar}H), 123.7 (NCHCHN), 122.5 (NCHCHN), 121.0 (q, J=321.3 Hz, CF₃), 50.7 (NCH₂), 31.7 (CH₂), 30.0 (CH₂), 29.2 (CH₂), 29.1 (CH₂), 28.8 (CH₂), 26.1 (CH₂), 22.6 (CH₂), 17.2 (CH_{3(ar)}), 14.0 (CH₃). ¹⁹F NMR (CDCl₃, 282.4 MHz): δ -79.5. Calc. for C₂₁H₂₉F₆N₃O₄S₂: C: 44.6%, H: 5.17%, N: 7.43%, S: 11.34%. Found: C: 44.47%, H: 5.38%, N: 7.29%, S: 11.07%.

1-(2-methylphenyl)-3-undecyl-1H-imidazolium bis(trifluoromethylsulfonyl)imide (2e)

The product was obtained as a brown liquid (589 g, 992 mmol, 95 %).

¹H NMR (CDCl₃, 300.13 MHz): δ 8.87 (s, 1 H, NCHN), 7.46 - 7.56 (m, 2 H, H_{ar}), 7.32 - 7.46 (m, 4 H, NCHCHN + H_{ar}), 4.36 (t, J=7.46 Hz, 2 H, NCH₂), 2.22 (s, 3 H, CH_{3,ar}), 1.97 (d, J=6.61 Hz, 2 H, CH₂), 1.57 (d, J=8.88 Hz, 2 H, CH₂), 1.23 - 1.37 (m, 14 H, CH₂), 0.84 - 0.91 (m, 3 H, CH₃). ¹³C NMR (CDCl₃, 75.475 MHz): δ 136.1 (NCHN), 133.4 (NC_{ar}), 133.2 (C_{ar}), 132.0 (C_{ar}H), 131.4 (C_{ar}H), 127.9 (C_{ar}H), 126.3 (C_{ar}H), 123.7 (NCHCHN), 122.5 (NCHCHN), 119.7 (q, J=321.3 Hz, CF₃), 50.7 (NCH₂), 31.9 (CH₂), 30.1 (CH₂), 29.5 (CH₂), 29.4 (CH₂), 29.3 (CH₂), 29.3 (CH₂), 28.9 (CH₂), 26.1 (CH₂), 22.6 (CH₂), 17.2 (CH_{3,ar}), 14.1 (CH₃). ¹⁹F NMR (CDCl₃, 282.4 MHz): δ -79.6. Calc. for C₂₃H₃₃F₆N₃O₄S₂: C: 46.53%, H: 5.60%, N: 7.08%, S: 10.80%; Found: C: 46.58%, H: 5.77%, N: 7.38%, S: 10.74%.

1-(4-methoxyphenyl)-3-pentyl-1H-imidazolium bis(trifluoromethylsulfonyl)imide (3b)

The product was obtained as a brown oil (68.5 g, 130 mmol, 92 %).

¹H NMR (CDCl₃, 300.13 MHz): δ 9.01 (s, 1 H, NCHN), 7.54 (s, 1 H, NCHCHN), 7.44 - 7.52 (m, 3 H, NCHCHN + H_{ar}), 7.05 (d, J=8.69 Hz, 2 H, H_{ar}), 4.30 (t, J=7.37 Hz, 2 H, NCH₂) 3.83 - 3.90 (m, 3 H, OCH₃), 1.87 - 2.01 (m, 2 H, CH₂), 1.33 - 1.44 (m, 4 H, CH₂), 0.91 (t, J=6.61 Hz, 3 H,

CH_3). ^{13}C NMR (CDCl_3 , 75.48 MHz): δ 161.1 (NC_{ar}), 134.1 (NCHN), 127.2 ($\text{C}_{\text{ar}}\text{OCH}_3$), 123.7 ($\text{C}_{\text{ar}}\text{H}$), 122.9 (NCHCHN), 121.9 (NCHCHN), 119.8 (q, $J=320.2$ Hz, CF_3), 115.6 ($\text{C}_{\text{ar}}\text{H}$), 55.8 (OCH_3), 50.6 (NCH₂), 29.8 (CH₂), 28.2 (CH₂), 21.9 (CH₂), 13.7 (CH₃). ^{19}F NMR (CDCl_3 , 282.4 MHz): δ – 79.5. Calc. for $\text{C}_{17}\text{H}_{21}\text{F}_6\text{N}_3\text{O}_5\text{S}_2$: C: 38.86%, H: 4.03%, N: 8.00%, S: 12.20%; Found: C: 38.68%, H: 4.12%, N: 8.30%, S: 12.35%.

*1-(4-methoxyphenyl)-3-octyl-1*H*-imidazolium bis(trifluoromethylsulfonyl)imide (3c)*

The product was obtained as a brown oil (10.8 g, 19.0 mmol, 95 %).

^1H NMR (CDCl_3 , 300.13 MHz): δ 9.00 (s, 1 H, NCHN), 7.57 (t, $J=1.70$ Hz, 1 H NCHCHN), 7.46 - 7.53 (m, 3 H, NCHCHN + H_{ar}), 7.00 - 7.08 (m, 2 H, H_{ar}), 4.28 (t, $J=7.55$ Hz, 2 H, NCH₂), 3.85 (s, 3 H, OCH₃), 1.92 (t, $J=6.99$ Hz, 2 H, CH₂), 1.24 - 1.37 (m, 10 H, CH₂), 0.83 - 0.90 (m, 3 H, CH₃). ^{13}C NMR (CDCl_3 , 75.48 MHz): δ 161.1 (NC_{ar}), 133.9 (NCHN), 127.2 ($\text{C}_{\text{ar}}\text{OCH}_3$), 123.7 ($\text{C}_{\text{ar}}\text{H}$), 122.9 (NCHCHN), 121.9 (NCHCHN), 119.9 (q, $J=346.1$ Hz, CF_3), 115.6 ($\text{C}_{\text{ar}}\text{H}$), 55.7 (OCH₃), 50.6 (NCH₂), 31.6 (CH₂), 30.1 (CH₂), 28.9 (CH₂), 28.8 (CH₂), 26.1 (CH₂), 22.5 (CH₂), 14.0 (CH₃). ^{19}F NMR (CDCl_3 , 282.4 MHz): δ – 79.6. Calc. for $\text{C}_{20}\text{H}_{27}\text{F}_6\text{N}_3\text{O}_5\text{S}_2$: C: 42.32%, H: 4.79%, N: 7.40%, S: 11.30%; Found: C: 42.60%, H: 4.97%, N: 7.54%, S: 11.19%.

*1-(4-methoxyphenyl)-3-nonyl-1*H*-imidazolium bis(trifluoromethylsulfonyl)imide (3d)*

The product was obtained as a brown oil (81.7 g, 141 mmol, 91 %).

^1H NMR (CDCl_3 , 300.13 MHz): δ 9.02 (s, 1 H, NCHN), 7.54 (s, 1 H, NCHCHN), 7.49 (d, $J=8.66$ Hz, 2 H, H_{ar}), 7.46 (s, 1 H, NCHCHN), 7.05 (d, $J=8.66$ Hz, 2 H, H_{ar}), 4.27 - 4.33 (m, 2 H, NCH₂), 3.86 (s, 3 H, OCH₃), 1.90 - 1.96 (m, 2 H, CH₂), 1.23 - 1.38 (m, 12 H, CH₂), 0.86 - 0.89 (m, 3 H, CH₃). ^{13}C NMR (CDCl_3 , 151 MHz): δ 161.2 (NC_{ar}), 134.2 (NCHN), 127.2 ($\text{C}_{\text{ar}}\text{OCH}_3$), 123.8 ($\text{C}_{\text{ar}}\text{H}$), 122.8 (NCHCHN), 121.9 (NCHCHN), 119.8 (q, $J=321.4$ Hz, CF_3), 115.6 ($\text{C}_{\text{ar}}\text{H}$), 55.8 (OCH₃), 50.7 (NCH₂), 31.7 (CH₂), 30.1 (CH₂), 29.2 (CH₂), 29.1 (CH₂), 28.9 (CH₂), 26.2 (CH₂), 22.6 (CH₂), 14.0 (CH₃). ^{19}F NMR (CDCl_3 , 282.4 MHz): δ – 79.5. Calc. for $\text{C}_{21}\text{H}_{29}\text{F}_6\text{N}_3\text{O}_5\text{S}_2$: C: 43.37%, H: 5.03%, N: 7.22%, S: 11.03%; Found: C: 43.73%, H: 5.14%, N: 7.23%, S: 10.65%.

*1-(4-methoxyphenyl)-3-undecyl-1*H*-imidazolium bis(trifluoromethylsulfonyl)imide (3e)*

The product was obtained as a brown oil (85.6 g, 140 mmol, 91 %).

^1H NMR (CDCl_3 , 300.13 MHz): δ 9.02 (s, 1 H, NCHN), 7.54 (s, 1 H, NCHCHN), 7.43 - 7.52 (m, 3 H, NCHCHN + H_{ar}), 7.00 - 7.09 (m, 2 H, H_{ar}), 4.30 (t, $J=7.55$ Hz, 2 H, NCH₂), 3.86 (s, 3 H, OCH₃), 1.86 - 1.99 (m, 2 H, CH₂), 1.21 - 1.36 (m, 16 H, CH₂), 0.84 - 0.89 (m, 3 H, CH₃). ^{13}C NMR (CDCl_3 , 75.48 MHz): δ 161.2 (NC_{ar}), 134.1 (NCHN), 127.2 ($\text{C}_{\text{ar}}\text{OCH}_3$), 123.7 ($\text{C}_{\text{ar}}\text{H}$), 122.8 (NCHCHN), 121.9 (NCHCHN), 119.8 (q, $J=320.8$ Hz, CF_3), 115.6 ($\text{C}_{\text{ar}}\text{H}$), 55.8 (OCH₃), 50.6 (NCH₂), 31.8 (CH₂), 30.1 (CH₂), 29.5 (CH₂), 29.4 (CH₂), 29.3 (CH₂), 29.3 (CH₂), 28.9 (CH₂), 26.2 (CH₂), 22.6 (CH₂), 14.1 (CH₃). ^{19}F NMR (CDCl_3 , 282.4 MHz): δ – 79.5. Calc. for $\text{C}_{23}\text{H}_{33}\text{F}_6\text{N}_3\text{O}_5\text{S}_2$: 45.31 %, H: 5.46%, N: 6.89%, S: 10.52%; Found: C: 45.69%, H: 5.76%, 7.08%, S: 10.41%.

1-(2,4-dimethylphenyl)-3-pentyl-1H-imidazolium bis(trifluoromethylsulfonyl)imide (4b**)**

The product was obtained as an orange liquid (345 g, 659 mmol, 87 %).

¹H NMR (CDCl₃, 300.13 MHz): δ 8.78 (s, 1 H, NCHN), 7.52 - 7.57 (m, 1 H, NCHCH), 7.33 (t, J=1.79 Hz, 1 H, NCHCH), 7.10 - 7.25 (m, 3 H, H_{ar}), 4.32 (t, J=7.46 Hz, 2 H, NCH₂), 2.39 (s, 3 H, CH_{3,ar}), 2.16 (s, 3 H, CH_{3,ar}), 1.94 (quin, J=7.46 Hz, 2 H, CH₂), 1.30 - 1.41 (m, 4 H, CH₂), 0.91 (t, J=6.80 Hz, 3 H, CH₃). ¹³C NMR (CDCl₃, 75.475 MHz): δ 141.8 (NC_{ar}), 135.8 (NCHN), 132.8 (C_{ar}), 132.5 (C_{arH}), 131.0 (C_{ar}), 128.3 (C_{arH}), 125.9 (C_{arH}), 123.9 (NCHCHN), 122.6 (NCHCHN), 119.7 (q, J=321.3 Hz, CF₃), 50.5 (NCH₂), 29.7 (CH₂), 28.11 (CH₂), 26.1 (CH₂), 21.9 (CH₂), 21.1 (CH_{3,ar}), 17.1 (CH_{3,ar}), 13.7 (CH₃). ¹⁹F NMR (CDCl₃, 282.4 MHz): δ – 79.6. Calc. for C₁₈H₂₃F₆N₃O₄S₂: C: 41.30%, H: 4.43%, N: 8.03%, S: 12.25%; Found: C: 41.27%, H: 4.30%, N: 8.30%, S: 12.60%.

1-(2,4-dimethylphenyl)-3-nonyl-1H-imidazolium bis(trifluoromethylsulfonyl)imide (4d**)**

The product was obtained as an orange liquid (528 g, 911 mmol, 95 %).

¹H NMR (CDCl₃, 300.13 MHz): δ 8.81 (s, 1 H, NCHN), 7.50 (s, 1 H, NCHCHN), 7.32 (s, 1 H, NCHCHN), 7.12 - 7.25 (m, 3 H, H_{ar}), 4.30 - 4.40 (m, 2 H, NCH₂), 2.40 (s, 3 H, CH_{3,ar}), 2.17 (s, 3 H, CH_{3,ar}), 1.94 (t, J=6.70 Hz, 2 H, CH₂), 1.37 - 1.20 (m, 12 H, CH₂), 0.86 - 0.90 (m, 3 H, CH₂). ¹³C NMR (CDCl₃, 75.475 MHz): δ 141.8 (NC_{ar}), 136.1 (NCHN), 132.8 (C_{ar}), 132.5 (C_{arH}), 131.0 (C_{ar}), 128.4 (C_{arH}), 126.0 (C_{arH}), 123.8 (NCHCHN), 122.4 (NCHCHN), 119.8 (q, J=321.3 Hz, CF₃), 50.7 (NCH₂), 31.7 (CH₂), 30.1 (CH₂), 29.2 (CH₂), 29.1 (CH₂), 28.8 (CH₂), 26.1 (CH₂), 22.6 (CH₂), 21.1 (CH_{3,ar}), 17.1 (CH_{3,ar}), 14.0 (CH₃). ¹⁹F NMR (CDCl₃, 282.4 MHz): δ – 79.6. Calc. for C₂₂H₃₁F₆N₃O₄S₂: C: 45.59%, H: 5.39%, N: 7.25%, S: 11.06%; found: C: 45.78%, H: 5.43%, N: 7.43%, S: 10.71%.

1-(2,4-dimethylphenyl)-3-undecyl-1H-imidazolium bis(trifluoromethylsulfonyl)imide (4e**)**

The product was obtained as a brown liquid (629 g, 1.04 mol, 94 %).

¹H NMR (CDCl₃, 300.13 MHz): δ 8.84 (s, 1 H, NCHN), 7.47 (s, 1 H, NCHCHN), 7.32 (s, 1 H, NCHCHN), 7.15 - 7.25 (m, 3 H, H_{ar}), 4.36 (t, J=7.46 Hz, 2 H, NCH₂), 2.41 (s, 3 H, CH_{3,ar}), 2.17 (s, 3 H, CH_{3,ar}), 1.95 (t, J=6.04 Hz, 2 H, CH₂), 1.29 - 1.40 (m, 6 H, CH₂), 1.26 (s, 10 H, CH₂), 0.85 - 0.90 (m, 3 H, CH₃). ¹³C NMR (CDCl₃, 75.475 MHz): δ 141.8 (NC_{ar}), 136.0 (NCHN), 132.8 (C_{ar}), 132.5 (C_{arH}), 131.0 (C_{ar}), 128.4 (C_{arH}), 126.0 (C_{arH}), 123.9 (NCHCHN), 121.9 (NCHCHN), 119.7 (q, J=321.3 Hz, CF₃), 50.6 (NCH₂), 31.9 (CH₂), 30.1 (CH₂), 29.5 (CH₂), 29.4 (CH₂), 29.3 (CH₂), 28.9 (CH₂), 26.1 (CH₂), 22.6 (CH₂), 21.1 (CH_{3,ar}), 17.1 (CH_{3,ar}), 14.1 (CH₃). ¹⁹F NMR (CDCl₃, 282.4 MHz): δ – Calc. for C₂₄H₃₅F₆N₃O₄S₂: C: 47.44%, H: 5.81%, N: 6.91%, S: 10.55%; Found: C: 47.50%, H: 6.11%, N: 6.94%, S: 10.59%.

2 TG curves

The TAAILs and metal precursors have to suitable for the microwave irradiation at 230 °C. The decomposition temperatures were controlled by TGA (Table S1 and Fig. S1–S2).

Table S1 Thermogravimetric analysis of the TAAILs.^a

Ionic Liquid	decomposition temperature [°C]
[BMIm]NTf ₂ (1)	424
[Ph ₂ -Me_Im_C4]NTf ₂ (2a)	402
[Ph ₂ -Me_Im_C5]NTf ₂ (2b)	411
[Ph ₂ -Me_Im_C9]NTf ₂ (2d)	405
[Ph ₂ -Me_Im_C11]NTf ₂ (2e)	399
[Ph ₄ -OMe_Im_C5]NTf ₂ (3b)	426
[Ph ₄ -OMe_Im_C8]NTf ₂ (3c)	415
[Ph ₄ -OMe_Im_C9]NTf ₂ (3d)	414
[Ph ₄ -OMe_Im_C11]NTf ₂ (3e)	410
[Ph _{2,4} -Me_Im_C5]NTf ₂ (4b)	411
[Ph _{2,4} -Me_Im_C9]NTf ₂ (4d)	410
[Ph _{2,4} -Me_Im_C11]NTf ₂ (4e)	407

^a See thermogravimetric diagrams in Fig. S1 in Supp. Info.

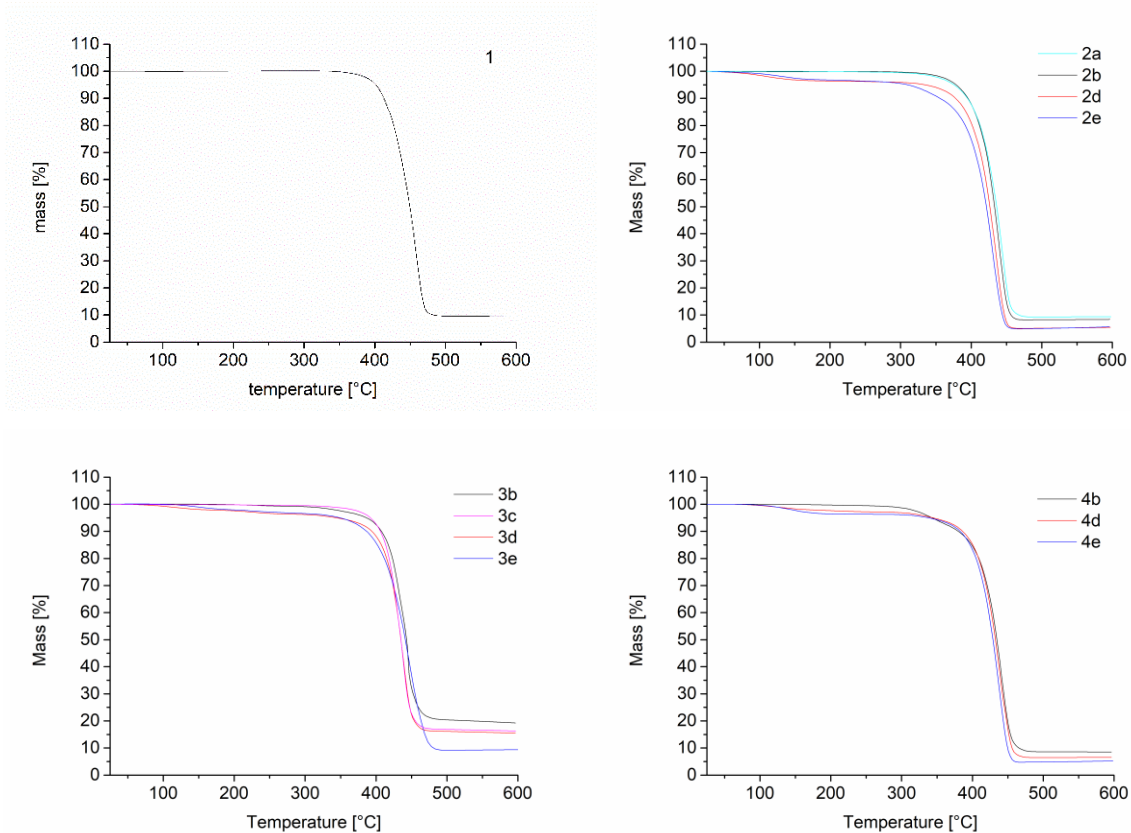


Fig. S1 TG curves of $[\text{BMIm}]\text{NTf}_2$ and the different TAAILs 2–4. 25–600 °C, heating rate 5 K/min.

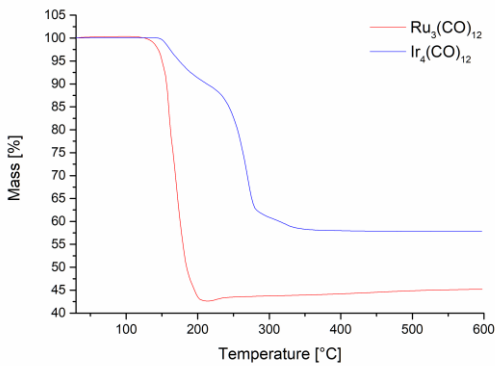


Fig. S2 TG curves of $\text{Ru}_3(\text{CO})_{12}$ and $\text{Ir}_4(\text{CO})_{12}$. 30–600 °C, heating rate 5 K/min.

3 Purity of the TAAILs

The anion purity and water content were determined by ion chromatography and *Karl Fischer titration* to be above 98.8 wt.-% (Table S2 and Fig. S3-S12).

Table S2 Purity of [BMIm]NTf₂ and the TAAILs.

Functionalized IL	IC [%] ^{a, b}	KFT [ppm] ^{c, d}
[BMIm]NTf ₂ (1)	99.9 (101% o. th.)	<10
[Ph ₂ -Me_Im_C4]NTf ₂ (2a)	99.9 (100% o. th.)	1648 ± 20
[Ph ₂ -Me_Im_C5]NTf ₂ (2b)	99.9 (97% o. th.)	770 ± 18
[Ph ₂ -Me_Im_C9]NTf ₂ (2d)	98.8 (96% o. th.)	117 ± 55
[Ph ₂ -Me_Im_C11]NTf ₂ (2e)	98.8 (97% o. th.)	313 ± 101
[Ph ₄ -OMe_Im_C5]NTf ₂ (3b)	99.4 (101% o. th.)	2289 ± 38
[Ph ₄ -OMe_Im_C9]NTf ₂ (3d)	99.3 (98% o. th.)	651 ± 21
[Ph ₄ -OMe_Im_C11]NTf ₂ (3e)	98.8 (99% o. th.)	764 ± 48
[Ph _{2,4} -Me_Im_C5]NTf ₂ (4b)	99.6 (90% o. th.)	1780 ± 35
[Ph _{2,4} -Me_Im_C9]NTf ₂ (4d)	98.8 (103% o. th.)	56 ± 56
[Ph _{2,4} -Me_Im_C11]NTf ₂ (4e)	98.8 (97% o. th.)	48 ± 48

^a Average bis(trifluoromethylsulfonyl)imide content and standard deviation (σ). ^b Sample preparation by dissolving a defined mass of IL in a defined volume of eluent. ^c Average water content and standard deviation (σ). ^d Measurement by using *Karl Fischer titration* with headspacemodeule, 170 °C.

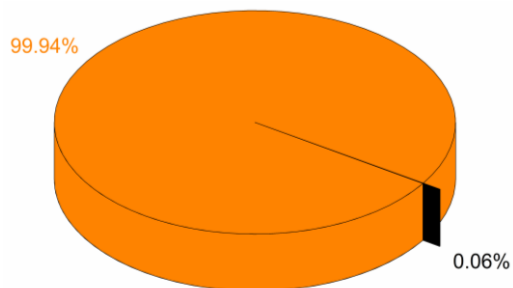


Fig. S3 Weight percent of anion in **2a**. Black: F⁻, orange: NTf₂⁻.

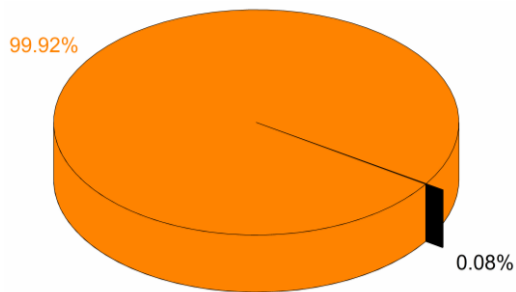


Fig. S4 Weight percent of anion in **2b**. Black: F⁻, red: Cl⁻, orange: NTf₂⁻.

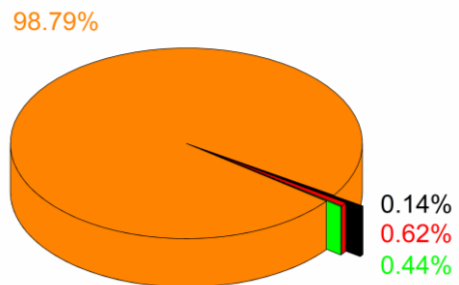


Fig. S5 Weight percent of anion in **2d**. Black: F⁻, red: Cl⁻, green: Br⁻, orange: NTf₂⁻.

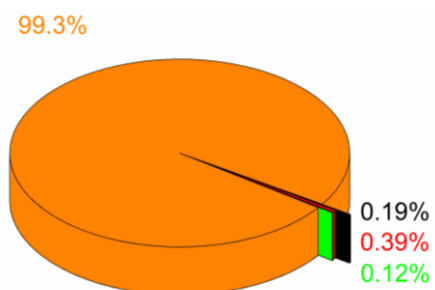


Fig. S6 Weight percent of anion in **2e**. Black: F⁻, red: Cl⁻, green: Br⁻, orange: NTf₂⁻.

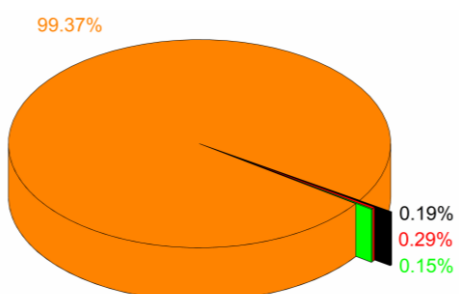


Fig. S7 Weight percent of anion in **3b**. Black: F⁻, red: Cl⁻, green: Br⁻, orange: NTf₂⁻.

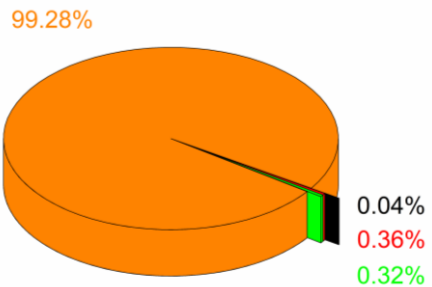


Fig. S8 Weight percent of anion in **3d**. Black: F⁻, red: Cl⁻, green: Br⁻, orange: NTf₂⁻.

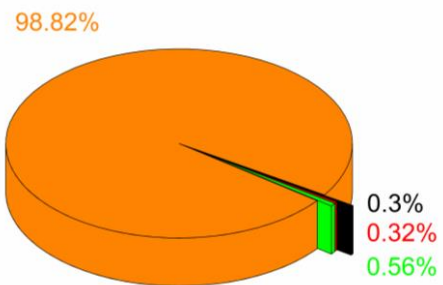


Fig. S9 Weight percent of anion in **3e**. Black: F⁻, red: Cl⁻, green: Br⁻, orange: NTf₂⁻.

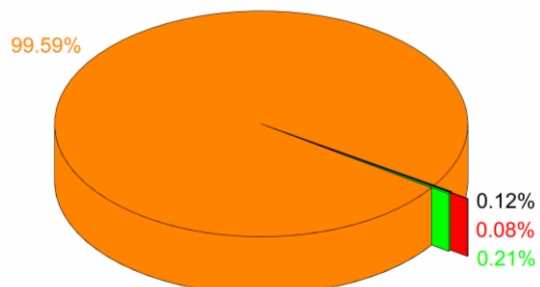


Fig. S10 Weight percent of anion in **4b**. Red: Cl⁻, green: Br⁻, orange: NTf₂⁻.

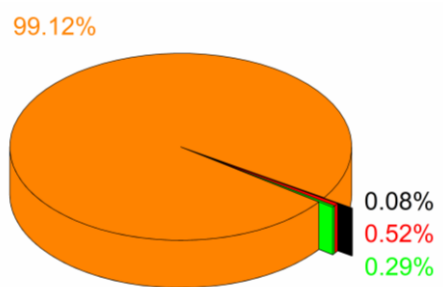


Fig. S11 Weight percent of anion in **4d**. Black: F⁻, red: Cl⁻, green: Br⁻, orange: NTf₂⁻.

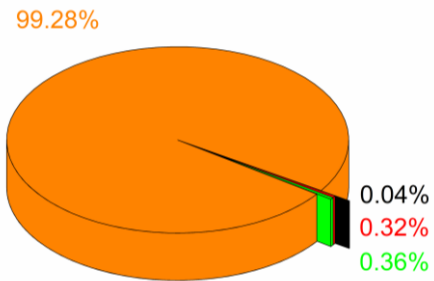


Fig. S12 Weight percent of anion in **4e**. Black: F⁻, red: Cl⁻, green: Br⁻ orange: NTf₂⁻.

4 Viscosity measurements

We investigate the viscosity of the TAAILs as a separation property for M-NPs (Table S3–S6).

Table S3 Viscosity measurements of [Ph₂-Me-Im-C4]NTf₂ (**2a**) from 20 °C to 80 °C.

T (°C)	Viscosity (cP)
20.2	418.6
25.2	305.1
30.2	222.3
35.2	162.8
40.1	122.8
45.2	89.07
50.2	72.55
55.3	57.9
60.1	47.44
65.3	38.14
70.2	32.56
75.2	27.21
79.8	23.49

Table S4 Viscosity measurements of [Ph₂-Me-Im-C5]NTf₂ (**2b**) from 20 °C to 80 °C.

T (°C)	Viscosity (cP)
20.2	437.2
24.9	320
30.3	222.3
35.1	163.7
40.3	119.1
45.2	94.88
50.2	74.42
55.3	60
59.6	48.83
65.1	39.3
69.8	33.02
75.1	27.67
80	23.49

Table S5 Viscosity measurements of [Ph₄-OMe-Im-C5]NTf₂ (**3b**) from 20 °C to 80 °C.

T (°C)	Viscosity (cP)
19.9	590.7
24.9	409.3
30.5	273.5
35.1	206.5
40	155.3
44.9	113.5
50.1	85.58
55.2	67.67
59.9	54.42
65.1	43.72
70.4	36.04
75	29.77
80.2	25.35

Table S6 Viscosity measurements of [Ph_{2,4-Me-Im-C5]NTf₂ (**4b**) from 20 °C to 80 °C.}

T (°C)	Viscosity (cP)
20.7	690.2
25.1	474.4
30.1	338.6
35.2	244.6
40.1	175.8
45.5	129.3
49.9	98.6
55.2	80.69
60.3	60.46
65.1	49.53
70.3	40.23
75.2	33.72
80.3	27.91

4.1 Xyz coordinates of optimized geometries of TAAIL cations

[BMIm]NTf₂ (1)

C	-2.31433900	1.14169400	-0.33051100
C	-1.03436200	1.39005300	0.06016500
C	-1.42014800	-0.76144800	0.33364300
N	-2.53767700	-0.21036500	-0.15305400
H	-3.07501300	1.80345200	-0.70876800
H	-0.47514900	2.30978600	0.08251000
H	-1.29122900	-1.80319500	0.57655800
C	-3.79485000	-0.91773200	-0.43962600
H	-4.59256000	-0.50626600	0.17804300
H	-4.04224800	-0.80465300	-1.49462500
H	-3.66691900	-1.97346200	-0.20942700
C	0.89917800	-0.02031400	0.94499600
H	0.91222200	-0.97575400	1.47211800
H	1.10641600	0.76193000	1.67770100
C	1.91618900	-0.00253700	-0.19798700
H	1.85789800	0.95587100	-0.72549300
H	1.65678900	-0.78066700	-0.92444700
C	3.34624100	-0.22251600	0.31494400
H	3.39799700	-1.17925700	0.84718700
H	3.59197400	0.55314400	1.04914300
C	4.38135000	-0.20722200	-0.81311900
H	4.38090000	0.75063700	-1.34082300
H	5.38645800	-0.36704800	-0.41821100
H	4.18365400	-0.99481200	-1.54565500
N	-0.49185800	0.18899700	0.47436300

[Ph₂-Me_Im_C5]NTf₂ (**2b**)

C	-0.48011700	-1.40855200	1.19268200
C	0.82938300	-1.09467400	1.38920100
C	0.17407600	-0.15273800	-0.49685900
N	-0.87175300	-0.81225300	0.00783300
H	-1.15700700	-1.99772300	1.78747100
H	1.50720200	-1.35103400	2.18495800
H	0.18353000	0.40891700	-1.41612800
C	-2.23404300	-0.85344200	-0.57527700
H	-2.13691800	-0.56275000	-1.62263700
H	-2.55817200	-1.89566500	-0.55198100
C	-3.21839000	0.05573000	0.16339200
H	-2.84273100	1.08473500	0.14284100
H	-3.27100400	-0.24149500	1.21645700
C	-4.61883500	-0.00284800	-0.46079100
H	-4.56127500	0.28985600	-1.51650100
H	-4.98228700	-1.03775200	-0.44724200
C	-5.62992000	0.89837100	0.25961200
H	-5.26442700	1.93183600	0.24733100
H	-5.68656000	0.60503900	1.31436400
N	1.22351900	-0.30695100	0.32164600
C	2.53974000	0.27380800	0.11604700
C	3.58129200	-0.53270100	-0.36220700
C	2.70408600	1.62529700	0.41235400
C	4.82184600	0.09200200	-0.53361900
C	3.95034100	2.21447300	0.22832900
H	1.86818500	2.20239000	0.79074800
C	5.00837300	1.44127600	-0.24416100
H	5.65335900	-0.49465900	-0.90706700
H	4.09158400	3.26374800	0.45538800
C	-7.02688500	0.84147200	-0.36359900
H	-7.43453800	-0.17322700	-0.33385900
H	-7.72133300	1.49267000	0.17166700
H	-7.00950900	1.16365000	-1.40889200
C	3.39939400	-1.99623500	-0.68033100
H	3.32182800	-2.60056800	0.22896400
H	2.50001000	-2.18052200	-1.27385700
H	4.25209900	-2.37065800	-1.24648700
H	5.98354500	1.89020400	-0.39052900

[Ph₄OMe_Im_C5]NTf₂ (**3b**)

C	-1.27975400	1.92506300	-0.58901100
C	0.04872200	1.80318200	-0.85860800
C	-0.50383800	0.23270400	0.59141000
N	-1.60763200	0.93434800	0.31676300
H	-2.01004200	2.62118700	-0.96448300
H	0.69169500	2.36007400	-1.51770200
H	-0.43510300	-0.58981100	1.28308100
C	-2.96022900	0.66691300	0.85927300
H	-2.82574400	0.06140100	1.75714500
H	-3.37384600	1.62806000	1.17046700
C	-3.87193100	-0.03402800	-0.15026700
H	-3.40865900	-0.97765200	-0.45895500
H	-3.96288500	0.58341300	-1.05052500
C	-5.26420400	-0.30158900	0.43630500
H	-5.16827000	-0.91476900	1.34089800
H	-5.71577400	0.64650700	0.75326300
C	-6.20291400	-1.00357800	-0.55334400
H	-5.74946800	-1.94971300	-0.87105200
H	-6.29812400	-0.39001900	-1.45675300
N	0.52057800	0.73669700	-0.11167500
C	1.87649500	0.24335500	-0.08828300
C	2.91649600	1.11006200	0.22714600
C	2.12821800	-1.09863400	-0.38683000
C	4.22684900	0.64087400	0.24716900
C	3.42794100	-1.56992700	-0.35688300
H	1.31718900	-1.76321700	-0.66168500
C	4.49095900	-0.70580300	-0.04160900
H	5.02584100	1.32405500	0.49802100
H	3.65211700	-2.60313200	-0.58937500
C	-7.59151400	-1.27210700	0.03221400
H	-8.08559200	-0.34160100	0.32662400
H	-8.23402200	-1.77157300	-0.69615300
H	-7.53291900	-1.91307700	0.91675800
H	2.71311000	2.14559200	0.47430200
O	5.71472900	-1.26317700	-0.04638000
C	6.86038200	-0.45700500	0.25068900
H	6.80125200	-0.05144300	1.26455900
H	7.71355000	-1.12662900	0.17634400
H	6.96717000	0.35356500	-0.47558000

[Ph_{2,4-Me}_Im_C5]NTf₂ (**4b**)

C	0.97810700	1.52584900	1.16430300
C	-0.34474700	1.29354700	1.38380300
C	0.23374700	0.25372200	-0.47492400
N	1.32153900	0.86887500	-0.00334000
H	1.69425200	2.09517300	1.73179400
H	-0.99827500	1.61478500	2.17629700
H	0.18152800	-0.33709900	-1.37420400
C	2.67642900	0.81326700	-0.60118700
H	2.55047100	0.49503500	-1.63742800
H	3.05978900	1.83538100	-0.61560700
C	3.61698000	-0.12632100	0.15629000
H	3.18367300	-1.13247200	0.17310000
H	3.69906700	0.20075200	1.19856500
C	5.01073100	-0.16707200	-0.48401300
H	4.92375000	-0.48870600	-1.52925500
H	5.43217200	0.84544400	-0.50725100
C	5.97825800	-1.10138300	0.25377300
H	5.55507200	-2.11238400	0.27793000
H	6.06424700	-0.77932900	1.29811100
N	-0.79564500	0.49436300	0.34774700
C	-2.14491700	-0.01481400	0.17397100
C	-3.14178300	0.82302100	-0.34183400
C	-2.39620800	-1.33708700	0.53167100
C	-4.41571900	0.26505600	-0.48229900
C	-3.67547000	-1.85479500	0.37540100
H	-1.59835900	-1.95130600	0.93362200
C	-4.70823600	-1.05731600	-0.13128700
H	-5.20646000	0.88737900	-0.88796100
H	-3.87110800	-2.88467300	0.65083500
C	7.36848000	-1.14300000	-0.38555300
H	7.83292200	-0.15257000	-0.39209400
H	8.03176700	-1.81569100	0.16253000
H	7.32010000	-1.49567900	-1.41997900
C	-2.87676800	2.25564400	-0.73477400
H	-2.72895700	2.89463400	0.14148300
H	-1.98729700	2.35203100	-1.36344500
H	-3.72121200	2.66004100	-1.29260500
C	-6.10572000	-1.60230300	-0.27467100
H	-6.66018100	-1.48391200	0.66214900
H	-6.66191400	-1.07868200	-1.05389800
H	-6.09527700	-2.66690800	-0.51555700

5 IR spectra

Complete decomposition of the metal carbonyl was ascertained by the disappearance of the characteristic carbonyl stretches between 2057–1982 cm⁻¹ by attenuated total reflection infrared spectroscopy (ATR-IR) (Fig. S13-S26 in the ESI).

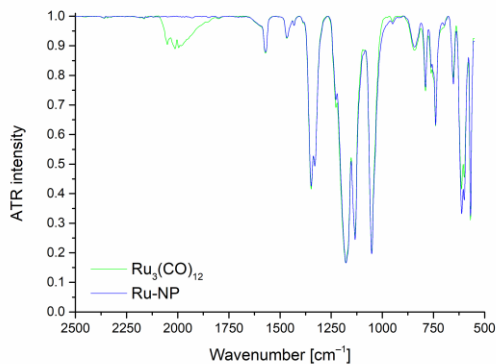


Fig. S13 ATR-IR spectra of $\text{Ru}_3(\text{CO})_{12}$ / IL **1** (green) and the resulting Ru-NP/ IL **1** dispersion (blue) after microwave irradiation.

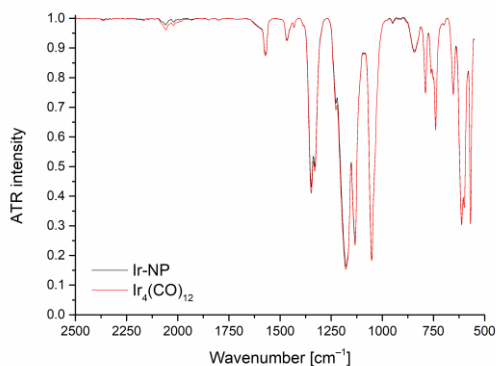


Fig. S14 ATR-IR spectra of $\text{Ir}_4(\text{CO})_{12}$ / IL **1** (red) and the resulting Ir-NP/ IL **1** dispersion (black) after microwave irradiation.

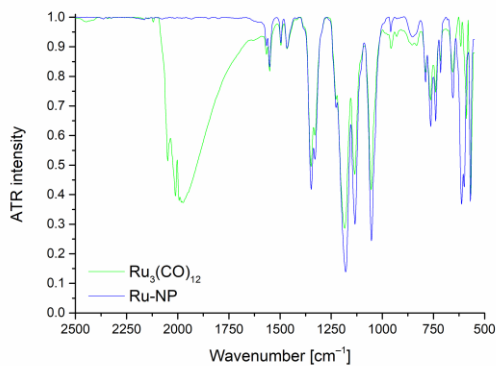


Fig. S15 ATR-IR spectra of $\text{Ru}_3(\text{CO})_{12}$ / TAAIL **2b** (green) and the resulting Ru-NP/ TAAIL **2b** dispersion (blue) after microwave irradiation.

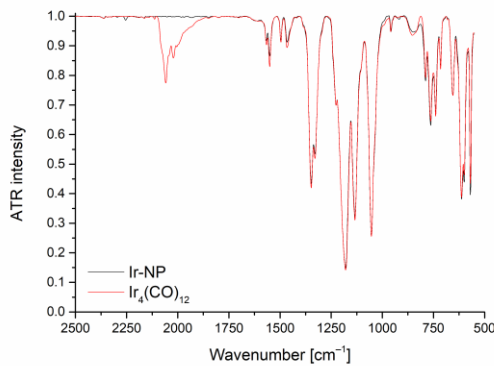


Fig. S16 ATR-IR spectra of $\text{Ir}_4(\text{CO})_{12}$ / TAAIL **2b** (red) and the resulting Ir-NP/ TAAIL **2b** dispersion (black) after microwave irradiation.

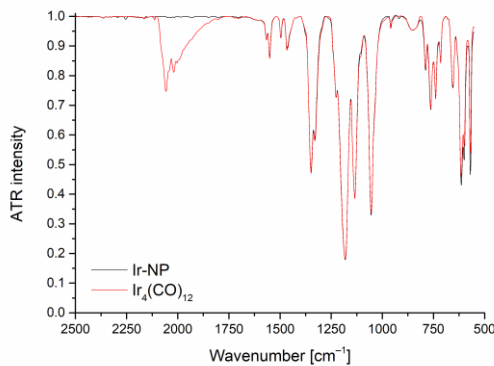


Figure S17 ATR-IR spectra of $\text{Ir}_4(\text{CO})_{12}$ / TAAIL **2d** (red) and the resulting Ir-NP/ TAAIL **2d** dispersion (black) after microwave irradiation.

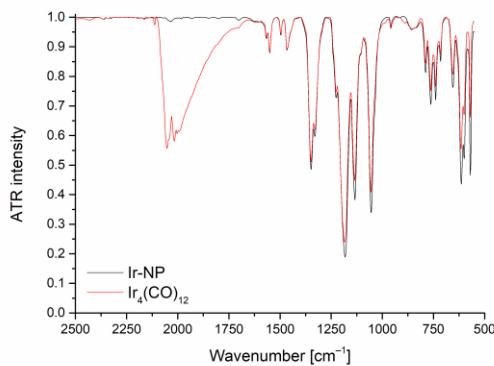


Fig. S18 ATR-IR spectra of $\text{Ir}_4(\text{CO})_{12}$ / TAAIL **2e** (red) and the resulting Ir-NP/ TAAIL **2e** dispersion (black) after microwave irradiation.

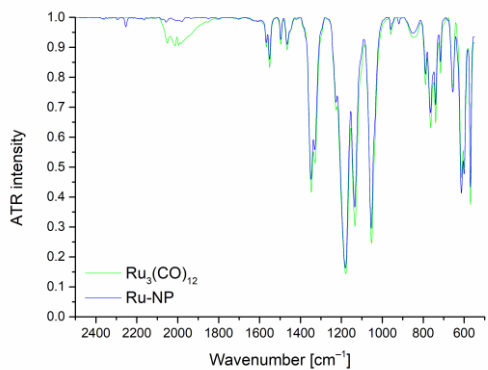


Fig. S19 ATR-IR spectra of $\text{Ru}_3(\text{CO})_{12}$ / TAAIL **2e** (green) and the resulting Ru-NP/ TAAIL **2e** dispersion (blue) after microwave irradiation.

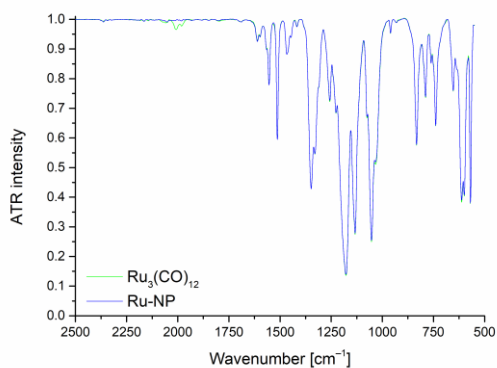


Fig. S20 ATR-IR spectra of $\text{Ru}_3(\text{CO})_{12}$ / TAAIL **3b** (green) and the resulting Ru-NP/ TAAIL **3b** dispersion (blue) after microwave irradiation.

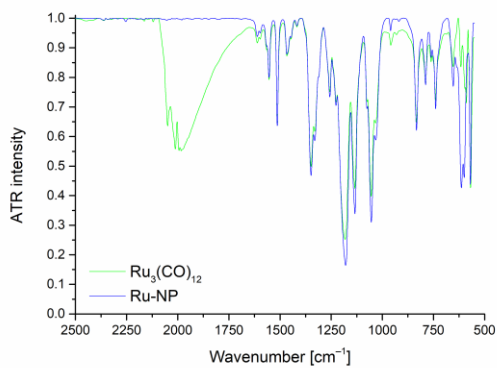


Fig. S21 ATR-IR spectra of $\text{Ru}_3(\text{CO})_{12}$ / TAAIL **3c** (green) and the resulting Ru-NP/ TAAIL **3c** dispersion (blue) after microwave irradiation.

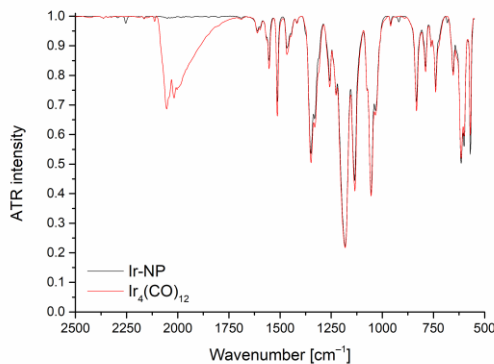


Fig. S22 ATR-IR spectra of $\text{Ir}_4(\text{CO})_{12}$ / TAAIL **3e** (red) and the resulting Ir-NP/ TAAIL **3e** dispersion (black) after microwave irradiation.

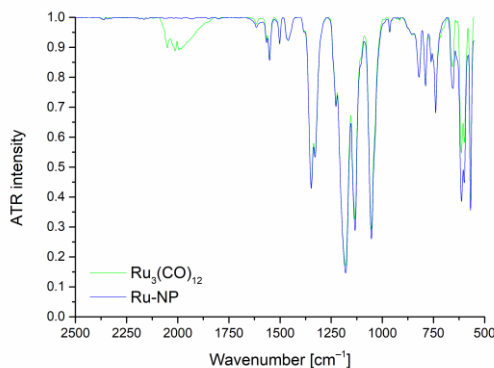


Fig. S23 ATR-IR spectra of $\text{Ru}_3(\text{CO})_{12}$ / TAAIL **4b** (green) and the resulting Ru-NP/ TAAIL **4b** dispersion (blue) after microwave irradiation.

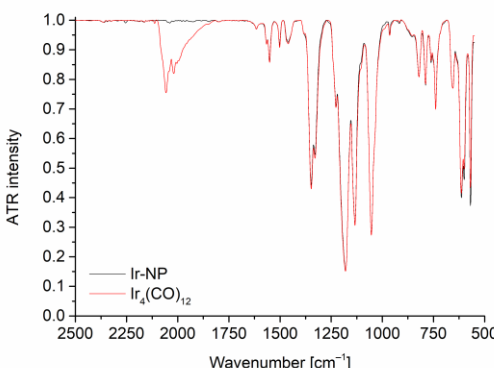


Fig. S24 ATR-IR spectra of $\text{Ir}_4(\text{CO})_{12}$ / TAAIL **4b** (red) and the resulting Ir-NP/ TAAIL **4b** dispersion (black) after microwave irradiation.

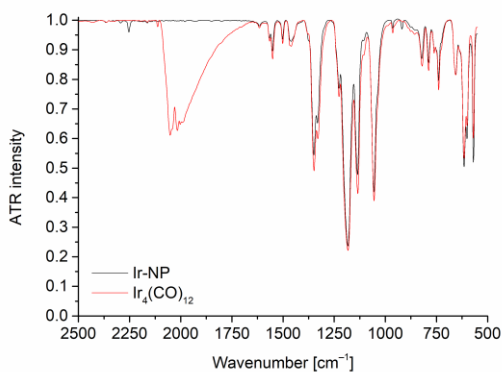


Fig. S25 ATR-IR spectra of Ir₄(CO)₁₂/ TAAIL **4d** (red) and the resulting Ir-NP/ TAAIL **4d** dispersion (black) after microwave irradiation.

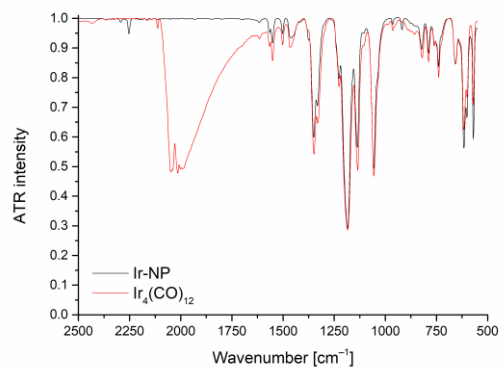


Fig. S26 ATR-IR spectra of Ir₄(CO)₁₂/ TAAIL **4e** (red) and the resulting Ir-NP/ TAAIL **4e** dispersion (black) after microwave irradiation.

6 TEM images

TEM images and histograms of the particle size for all M-NPs in TAAILs are shown in the following section (Fig. S27–S43).

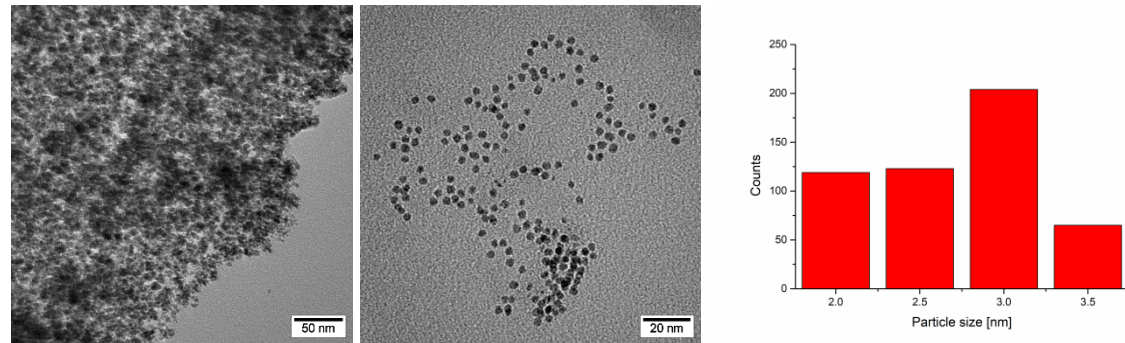


Fig. S27 Left, middle: TEM images of 1wt.-% Ru-NP in **1**; right: particle size histogram of Ru-NP in **1**.

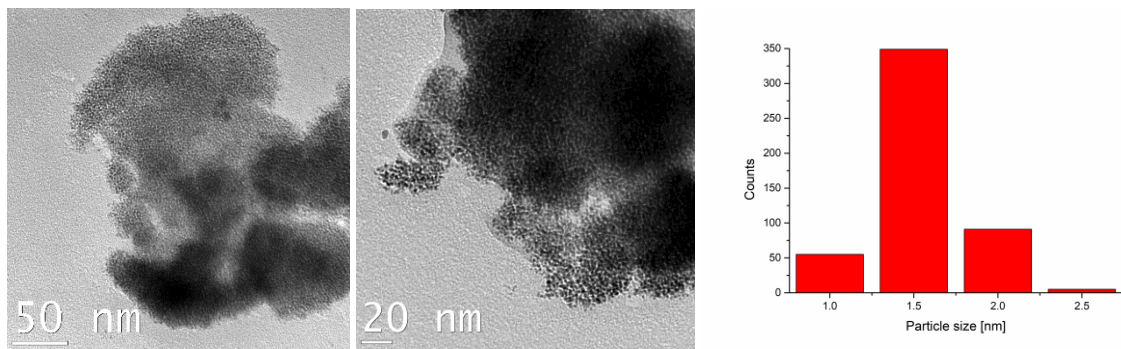


Fig. S28 Left, middle: TEM images of 0.5wt.-% Ir-NP in **1**; right: particle size histogram of Ir-NP in **1**.

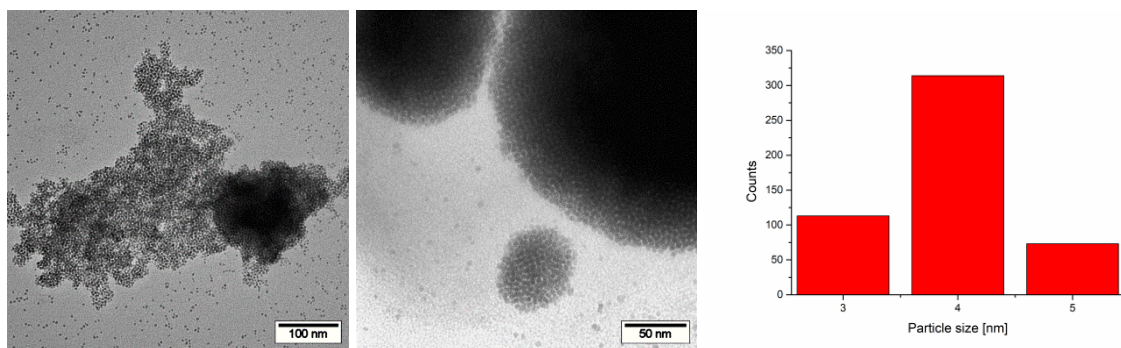


Fig. S29 Left, middle: TEM images of 1wt.-% Ru-NP in **2a**; right: particle size histogram of Ru-NP in **2a**.

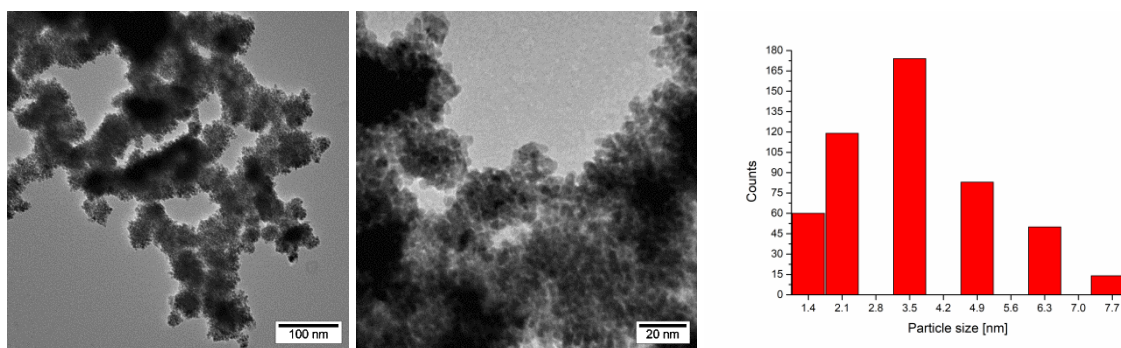


Fig. S30 Left, middle: TEM images of 1wt.-% Ru-NP in **2b**; right: particle size histogram of Ru-NP in **2b**.

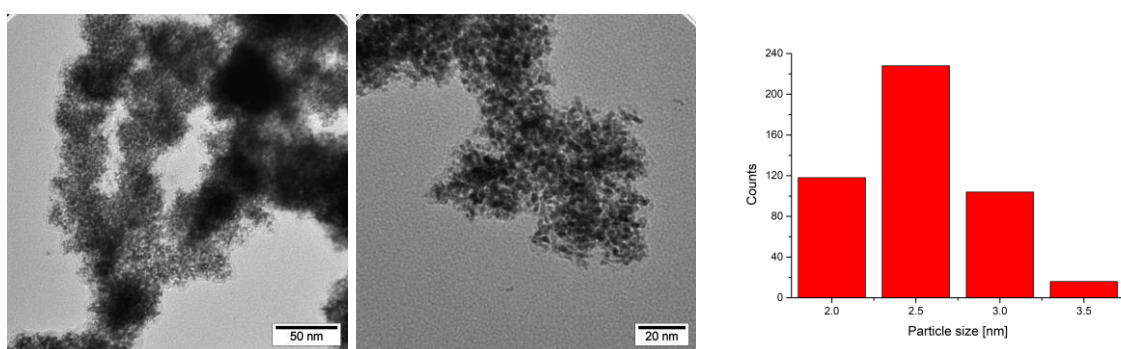


Fig. S31 Left, middle: TEM images of 1wt.-% Ir-NP in **2b**; right: particle size histogram of Ir-NP in **2b**.

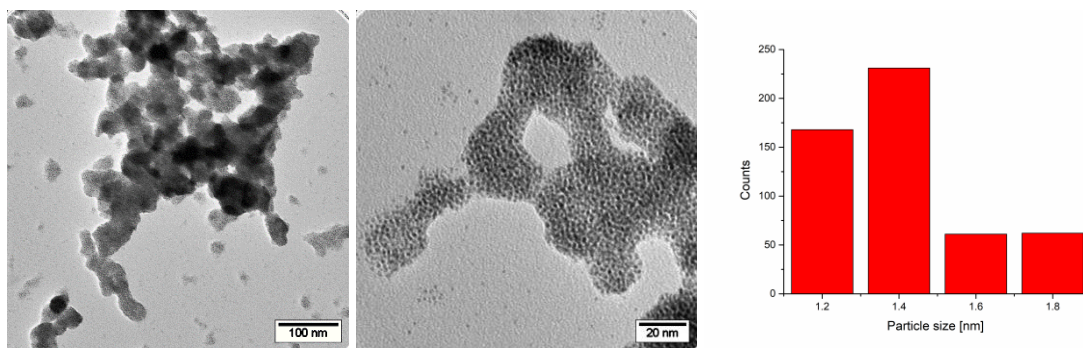


Fig. S32 Left, middle: TEM images of 1wt.-% Ir-NP in **2d**; right: particle size histogram of Ir-NP in **2d**.

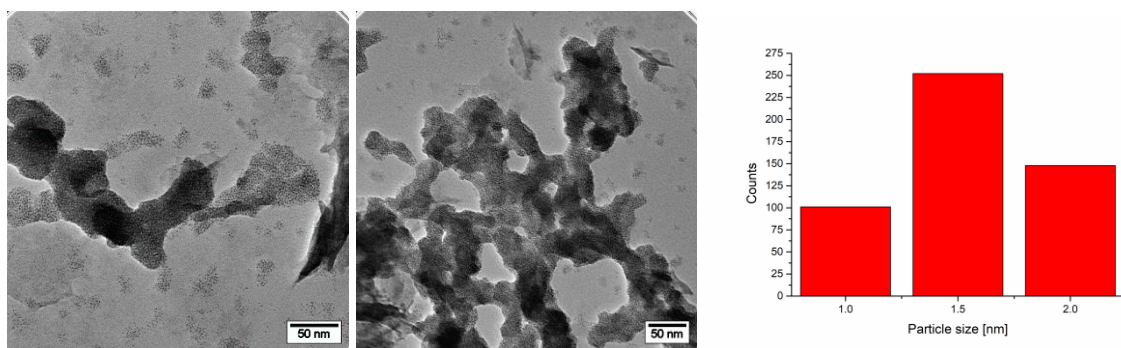


Fig. S33 TEM images of 1wt.-% Ir-NP in **2e**. right: particle size histogram of Ir-NP in **2e**.

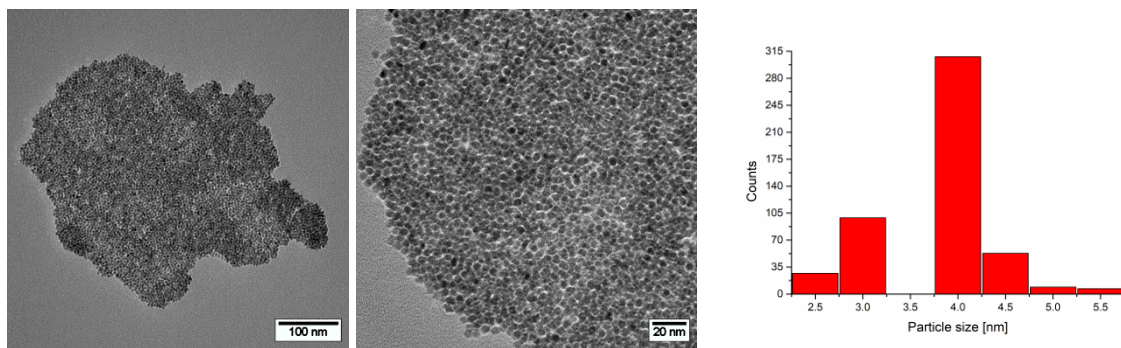


Fig. S34 Left, middle: TEM images of 1wt.-% Ru-NP in **3b**; right: particle size histogram of Ru-NP in **3b**.

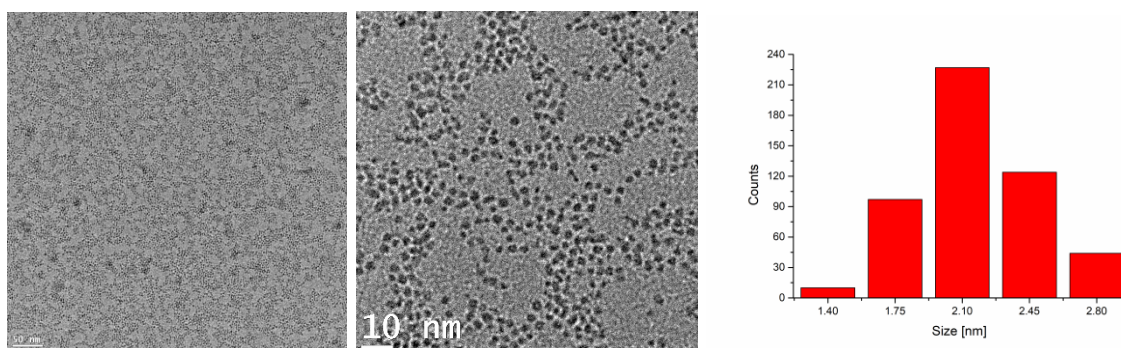


Fig. S35 Left, middle: TEM images of 1wt.-% Ru-NP in **3c**; right: particle size histogram of Ru-NP in **3c**.

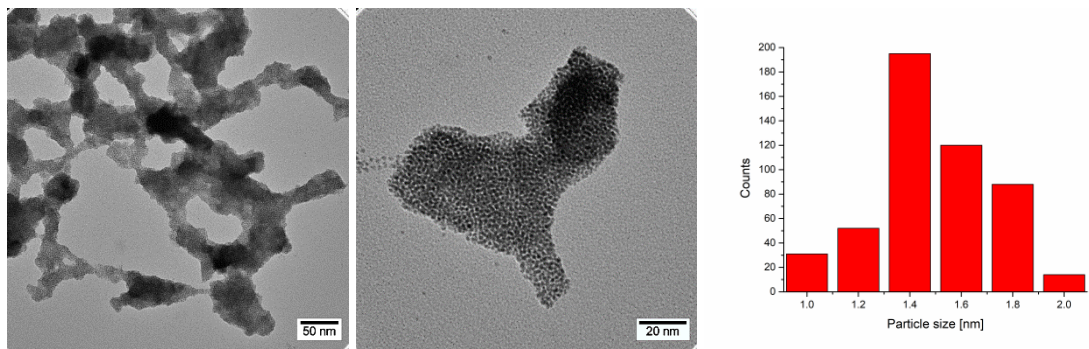


Fig. S36 Left, middle: TEM images of 1wt.-% Ir-NP in **3e**; right: particle size histogram of Ir-NP in **3e**.

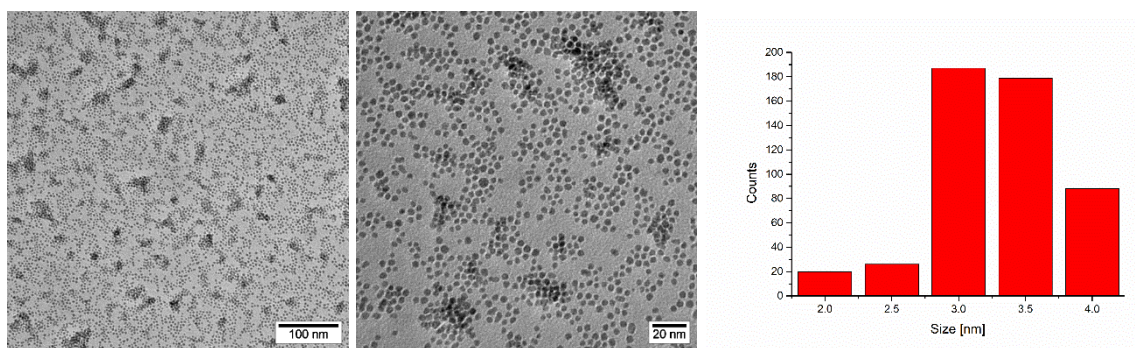


Fig. S37 Left, middle: TEM images of 1wt.-% Ru-NP in **4b**; right: particle size histogram of Ru-NP in **4b**.

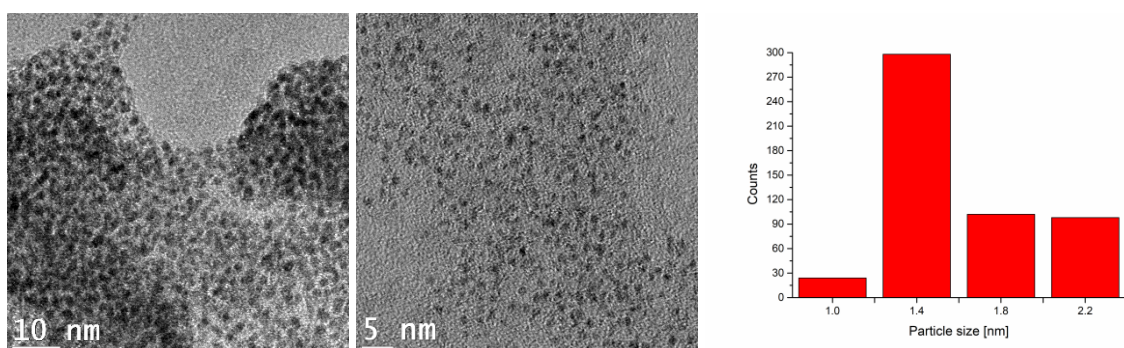


Fig. S38 Left, middle: TEM images of 1wt.-% Ir-NP in **4b**; right: particle size histogram of Ir-NP in **4d**.

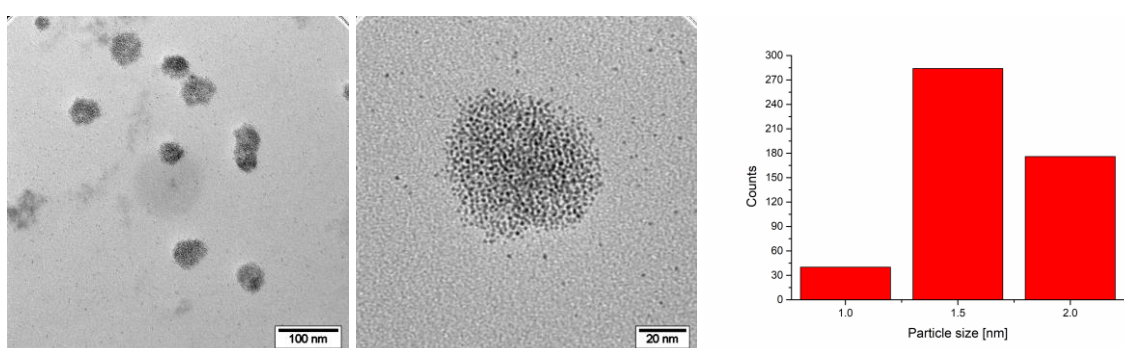


Fig. S39 Left, middle: TEM images of 1wt.-% Ir-NP in **4d**; right: particle size histogram of Ir-NP in **4d**.

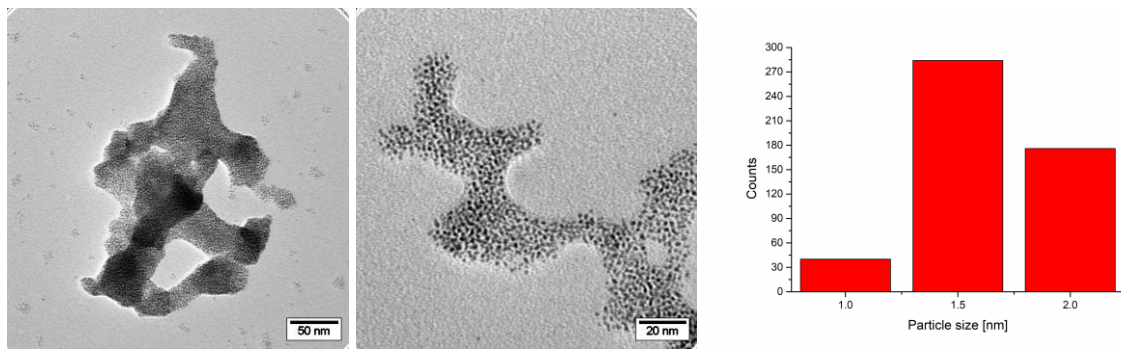


Fig. S40 Left, middle: TEM images of 1wt.-% Ir-NP in **4e**; right: particle size histogram of Ir-NP in **4e**.

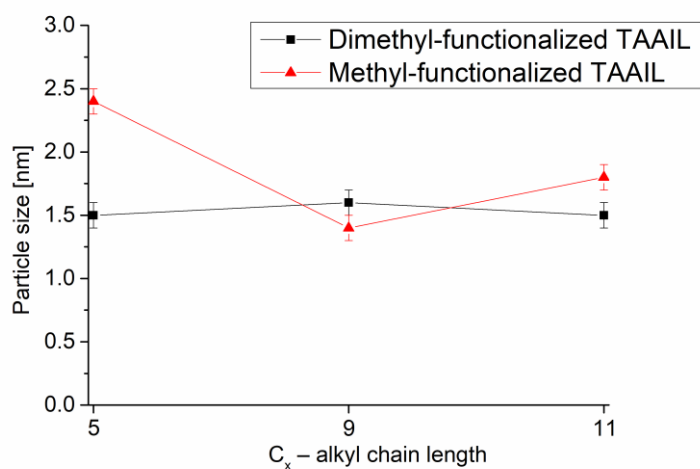


Fig. S41 Correlation between Ir-NP size and the alkyl chain length of the TAAILs methyl-functionalized TAAILs **2b**, **2d**, **2e** (red) and dimethyl-functionalized TAAILs **4b**, **4d**, **4e** (black). Errors bars indicate the standard deviation.

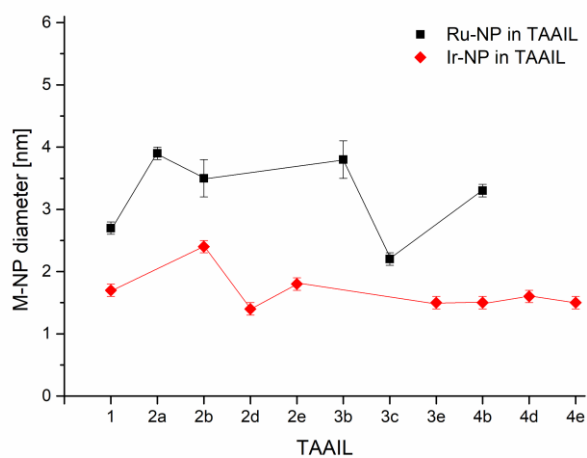


Fig. S42 Correlation between Ru-NP (black)/ Ir-NP (red) size and the different TAAILs. Errors bars indicate the standard deviation.

7 Selected area electron diffractions (SAED)

A face centred cubic phase could be obtained for all crystalline Ru- (COD: 1534914) and Ir- (COD: 1534947) NPs by SAED (Fig. S43–S50). The diffraction rings with the hkl indices (111), (200), (220), (311), (222) from inside to outside are shown exemplary in Fig. S49.

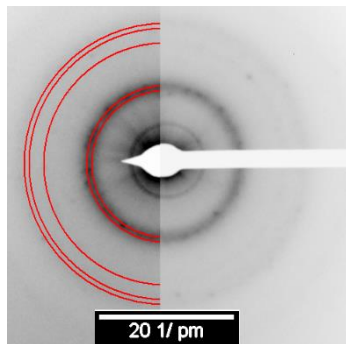


Fig. S43 SAED image of Ru-NP in 1.

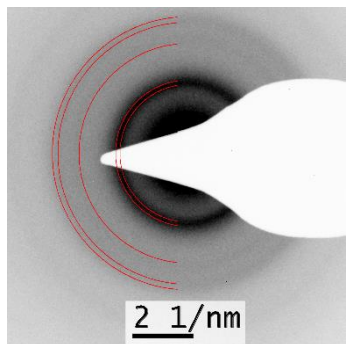


Fig. S44 SAED image of Ir-NP in 1.

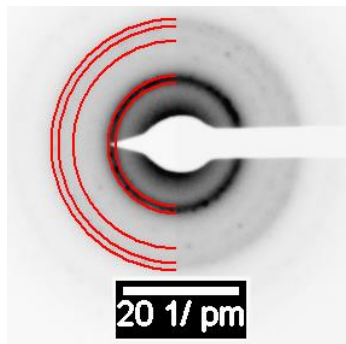


Fig. S45 SAED image of Ru-NP in 2a.

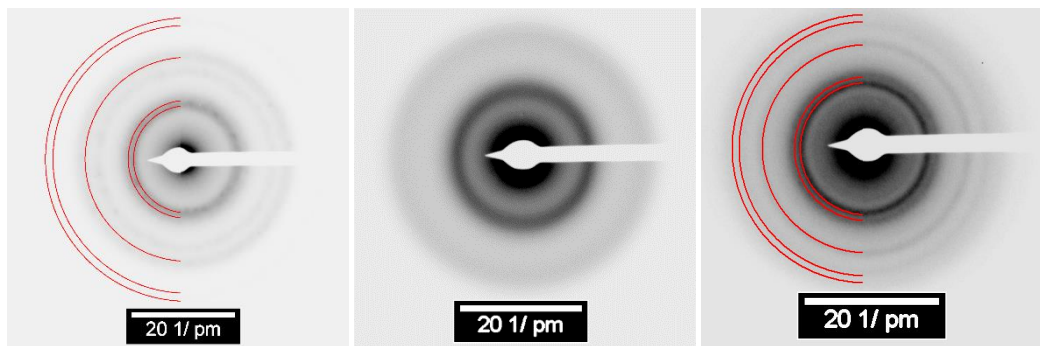


Fig. S46 SAED image of Ir-NP in **2b**, **2d**, **2e**.

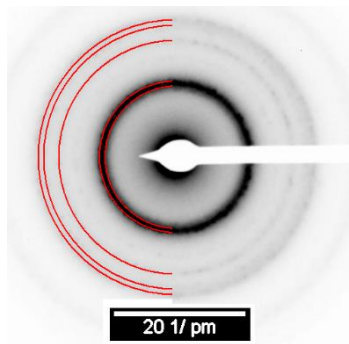


Fig. S47 SAED image of Ru-NP in **3b**.

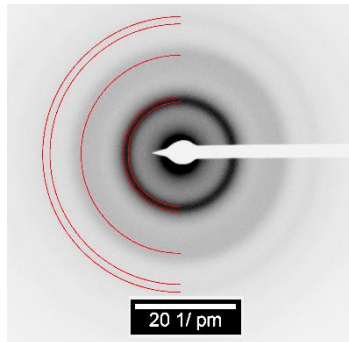


Fig. S48 SAED image of Ir-NP in **3e**.

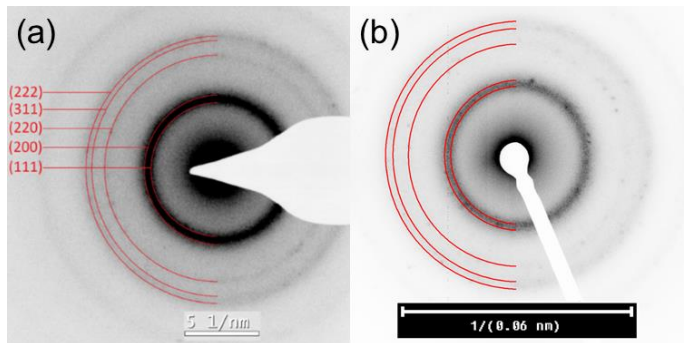


Fig. S49 SAED images of Ru-NP in **4b** before (a) and after (b) catalysis.

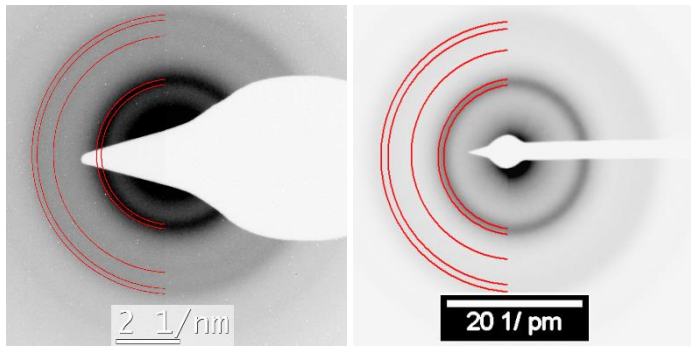


Fig. S50 SAED image of Ir-NP in **4b**, **4d**.

8 ε -ePC-SAFT

8.1 Density measurements of pure ILs

The liquid density of pure components or mixtures is an approved property for gaining pure-component parameters for the here used new equation of state in the electrolyte perturbed-chain statistical association fluid theory framework, ε -ePC-SAFT, incorporating a concentration-dependent dielectric constant. The model is utilized to validate the relationship between IL-solvent interactions and the already discussed agglomeration/aggregation effect of the synthesized NPs in different ILs. For the investigation, the four ILs **1b**, **3b**, **3e** and **4b** have been considered as they lead to different aggregation effects. The density plot for these ILs is shown in Fig. S51 in the next section. For general applicability to other structurally related ILs (see next section) also the density for the other ILs has been measured. Temperature-dependent density data can be found in Table S7–Table S9.

Table S7 Measured and modelled liquid density of 2-methyl TAAILs. All densities were measured at 1 bar and modelled with ε -ePC-SAFT.

T[K]	2b		2d		2e	
	ρ^{exp}	ρ^m	ρ^{exp}	ρ^m	ρ^{exp}	ρ^m
293.15	1396.2	1392.98	1276.3	1283.75	1247.1	1246.1
295.65	1393.9	1390.3	1274.2	1280.81	1245	1242.7
298.15	1391.5	1387.64	1272	1277.94	1243	1239.41
300.65	-	-	-	-	1240.7	1236.23
303.15	1386.8	1382.42	1267.7	1272.36	1238.8	1233.14
308.15	1382.1	1377.33	1263.3	1267.02	1234.6	1227.24
ARD%	0.2855		0.4463		0.3642	

Table S8 Measured and modelled liquid density of 4-methoxy TAAILs. All densities were measured at 1 bar and modelled with ε -ePC-SAFT.

T[K]	3b		3c		3c		3e	
	ρ^{exp}	ρ^m	ρ^{exp}	ρ^m	ρ^{exp}	ρ^m	ρ^{exp}	ρ^m
293.15	1398.5	1399.57	1324.1	1321.2	1303.7	1301.22	1266.5	1268.92
295.65	1396.2	1396.76	1321.9	1318.31	1301.5	1298.29	1264.3	1265.71
298.15	1393.8	1394.02	1319.7	1315.51	1299.4	1295.42	1262.2	1262.58
300.65	-	-	-	-	1297.2	1292.61	-	-
303.15	1391.5	1391.33	1315.2	1310.05	1295	1289.86	1257.9	1256.56
308.15	1389.2	1388.64	1310.8	1304.77	1290.6	1284.46	1253.6	1250.8
310.65	1384.5	1383.39	-	-	1288.5	1281.83	-	-
313.15	-	-	-	-	1286.3	1279.26	-	-
ARD%	0.04409		0.3321		0.3792		0.1326	

Table S9 Measured and modelled liquid density of 2,4-dimethyl TAAILs. All densities were measured at 1 bar and modelled with ε -ePC-SAFT.

T[K]	4b		4d		4e	
	ρ^{exp}	ρ^m	ρ^{exp}	ρ^m	ρ^{exp}	ρ^m
288.15	1348.5	1350.44	-	-	-	-
293.15	1343.9	1344.92	1263.4	1264.02	1230.4	1232.16
295.65	-	-	1261.2	1261.28	1228.3	1229.31
298.15	1339.4	1339.55	1259.2	1258.57	1226.2	1226.51
303.15	1334.8	1334.31	1257	1255.92	1222	1221.06
308.15	1330.2	1329.17	1254.8	1253.31	1217.9	1215.8
313.15	1325.7	1324.15	1250.5	1248.2	-	-
ARD%	0.07694		0.08237		0.09987	

8.2 Modelling with ε -ePC-SAFT

The new model ε -ePC-SAFT, a variation to the original ePC-SAFT⁴, was invented to account for the special properties of ILs. In the model, the Debye-Hückel term, accounting for the electrolyte contribution, was revised. The dielectric constant used to model the ion-ion interaction in a solvent, is here varied with the concentration of the electrolyte/IL. For further information, the reader may refer to recently published work.⁵ Following the modelling strategy proposed in a previous work⁶⁻⁸, ion-specific pure-component parameters for the ILs are obtained from straight fitting to directly measurable thermodynamic properties. For ILs, the use of pure-component liquid densities has been established as a reliable source for modelling. Briefly, ILs are described by three pure-component parameters for each IL-ion. These parameters are the segment number m^{seg} , the segment diameter σ_i as well as the dispersion-energy parameter u/k_B , with the Boltzmann constant k_B . These parameters allow ε -ePC-SAFT to explicitly account for interactions caused by hard-chain repulsion, van-der-Waals attraction and electrostatics. In accordance with previous work, where also the parameters of the NTf₂-anion have been obtained, the cations are fitted with respect to a linear molecular weight-

dependent ($M_{w,IL}$) equation for the three pure-component parameters (eq. S1). For this purpose, at least two ILs of a similar kind need to be modelled in order to receive a weight-dependent equation. This allows for characterizing structurally related cations, e.g. cations with changing alkyl chain length only.

$x = aM_w + b$	(eq. S1)
----------------	----------

The variables a and b in equation S1 are listed in Table S10 for each IL species and the corresponding pure-component parameters. The density measured and modelled are displayed in Table S7 to Table S9 with the respective ARD%.

For the ILs under investigation, the influence of the IL-solvent interactions on the agglomeration effect (**1b**, **3b**, **3e** and **4b**) and the fitted ϵ -ePC-SAFT parameters are listed in Table S11. The respective density plot is shown in Fig. S51.

Table S10 ePC-SAFT pure-component parameters for IL-ions of the ILs considered in this work. Parameters were fitted to pure liquid density data at 1 bar over a temperature range of 288.15 to 313.15 K.

IL-ion	a	b
Segment number m_{seg}		
1	0.0470	-18.7970
3	0.0516	-21.2270
4	0.0425	-15.7450
Segment diameter σ_i		
1	0.0005	3.5041
3	0.0000	3.6480
4	0.0010	3.0519
Dispersion energy u/k_B		
1	0.8338	194.9700
3	0.8081	128.6500
4	0.8890	29.0730

Table S11 ePC-SAFT pure-component parameters for IL-ions of the TAAILs considered in this work.

IL-ion	M _W [g mol ⁻¹]	m _{seg} [-]	σ [Å]	u/k _B [K]
Cation				
1b⁺	229.34890	5.17267	3.75949	619.77165
3b⁺	245.34830	5.88967	3.65001	553.31131
3e⁺	301.44750	8.78456	3.65022	598.64665
4b⁺	243.37570	6.46465	3.60288	495.58437
Anion				
[NTf ₂] ^{-[a]}	280.145	6.0103	3.7469	375.6529

[a] taken from reference 7, ARD = 100 · $\frac{1}{NP} \sum_{i=1}^{NP} \left| 1 - \frac{\rho^{calc}}{\rho^{exp}} \right|$.

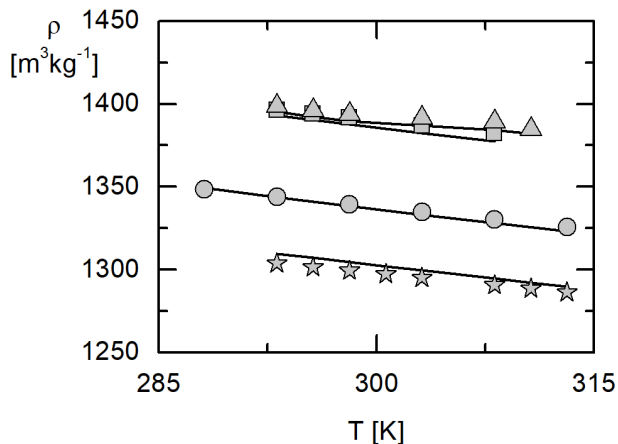


Fig. S51 Temperature-dependent density of the pure ILs considered for modelling in this work. Symbols: experimental data; Lines: ε-ePC-SAFT modelling results. Squares: [Ph₂-Me_Im_C5] (**2b**), Stars: [Ph₄-OMe_Im_C5] (**3b**), Triangles: [Ph₄-OMe_Im_C11] (**3e**), Circles: [Ph_{2,4}-Me_Im_C5] (**4b**).

With the obtained parameters, a solubility screening in different solvents was performed to give further insight into the structure-related hydrophobicity that could give hints on nanoparticle agglomeration. The screening included four solvents, namely water, acetonitrile (ACN), dichloromethane (DCM), and *n*-hexane. Their pure component parameters are available from literature and summarized in Table S12. As water is an associating compound, association energy and association volume are additionally needed. In ε-ePC-SAFT, the association is connected to an association scheme (2B for water), the location where the association originates.

Table S12 ε -ePC-SAFT pure-component parameters for solvents considered in this work.

Solvent	m_{seg}	σ	u/k_B	ε^{AiBj}	κ^{AiBj}	REF
	[-]	[Å]	[K]	[K]	[-]	
Water	1.2047	2.7927	353.9449	2425.6714	0.04509	9
ACN	3.3290	3.1898	311.31	-	-	10
DCM	2.2632	3.3380	274.20	-	-	11
Hexane	3.0577	3.7983	236.7691	-	-	12

In ε -ePC-SAFT, the mutual solubility of the IL and a solvent is calculated iteratively according to the isofugacity criterion following equation (eq. S2). Here, the product of the fugacity coefficient φ_i and the mole fraction x_i in phase I has to be equal to the product in the second phase II .

$$x_i^I \cdot \varphi_i^I = x_i^{II} \cdot \varphi_i^{II} \quad (\text{eq. S2})$$

In the iteration, the mole fraction is varied for both phases and is used as an input to ε -ePC-SAFT to allow calculating φ_i . The solubility is calculated when the isofugacity criterion is met. For the systems where immiscibility appeared, the mutual solubility of IL and solvent was quantified with ε -ePC-SAFT. The solubility of water in the IL was brought into order from high to low solubility. The series is: **3e > 3b > 1b > 4b**. The order of *n*-hexane solubility for the ILs was found to be: **4b < 1b < 3b < 3e**, the reversed order compared to the water solubility.

9 Catalysis

Based on the number of moles of the metal used, the turnover frequency (TOF) can be calculated as a measure of catalyst activity even though only the surface atoms of the Ru-NPs can be catalytically active. Even the TOF based on surface atoms will still be an understatement of the true activity of the active site because only a fraction of the surface atoms will be catalytically active, such as corners, edges, or defect sites.¹³ From TEM, we obtained an average Ru-NPs diameter of 3 nm for Ru/**4b** and 4 nm for Ru/**2b**. From these average diameters D the total number of metal atoms (N_T) in the nanocrystal can be calculated according to equation S3:¹³⁻¹⁶

$$N_T = \frac{N_A \rho V}{A_r} \text{ and } V = \frac{4}{3} \pi \left(\frac{D}{2} \right)^3 \quad (\text{eq. S3})$$

with N_A =Avogadro's number ($6.022 \cdot 10^{23} \text{ mol}^{-1}$), ρ = metal density, A_r = relative atom mass [$\text{g} \cdot \text{mol}^{-1}$]. N_T = 1042 atoms for Ru/**4b** and N_T = 2470, for Ru/**2b**.

Assuming that Ru clusters with more than 147 atoms have a cuboctahedral shell structure,¹⁷ it is possible to provide the number of shells (m) which can be derived from the total number of atoms (N_T).

The total average atom number $N_T = 1042$ is between the total atom number of $N_m = 923$ for a cuboctahedron with $m = 7$ shells and $N_m = 1415$ for a cuboctahedron with $m = 8$ shells according to $N_m = (1/3)(2m-1)(5m^2-5m+3)$.¹⁷

The number of shells can then be used to calculate the number of surface atoms (N_s) using eq. S4.¹⁸

$$N_s = 10m^2 - 20m + 12 \quad (\text{eq. S4})$$

The number of surface atoms for a seven-shell cuboctahedron is $N_s = 362$ and for an eight-shell cuboctahedron $N_s = 492$. In our approximation, we take here an average of $N_s = 430$ for the number of surface atoms for $N_T = 1042$. This gives a fraction of exposed or surface atoms $N_s/N_T \approx 430/1042 = 0.41$ or 41% on average.

The total average atom number $N_T = 2470$ is between the total atom number of $N_m = 2057$ for a cuboctahedron with $m = 9$ shells and $N_m = 2869$ for a cuboctahedron with $m = 10$ shells. The number of surface atoms for a nine-shell cuboctahedron is $N_s = 624$ and for a ten-shell cuboctahedron $N_s = 812$. In our approximation, we take here $N_s = 720$ for the number of surface atoms for $N_T = 2470$. This gives a fraction of exposed or surface atoms $N_s/N_T \approx 720/2470 = 0.29$ or 29% on average.

The H₂-uptake over time for the hydrogenation of benzene with Ru/**4b** and Ru/**1b** are given in Fig. S52 and Fig. S53.

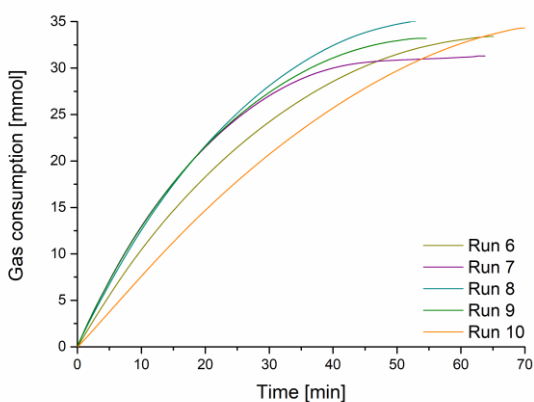


Fig. S52 H₂-uptake over time for the hydrogenation of benzene (0.91 g, 1.0 mL, 11.7 mmol) with Ru/**4b** (5.1 mg, 5.05·10⁻² mmol), 70 °C and 10 bar H₂.

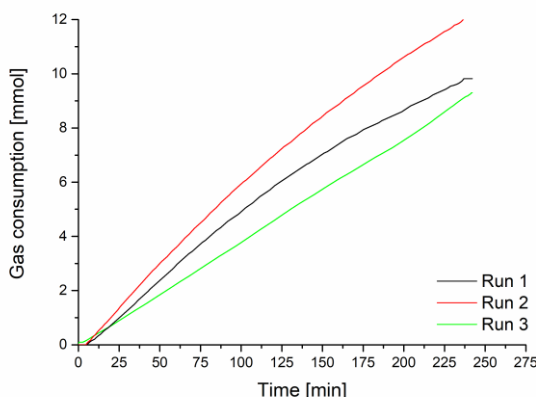


Fig. S53 H₂-uptake over time for the hydrogenation of benzene (0.91 g, 1.0 mL, 11.7 mmol) with Ru/**2b** (4.4 mg, $5.35 \cdot 10^{-2}$ mmol), 70 °C and 10 bar H₂.

At the end, the Ru-NPs were checked by TEM and PXRD for differences to the pre-catalysis state (Fig. S54-S55).

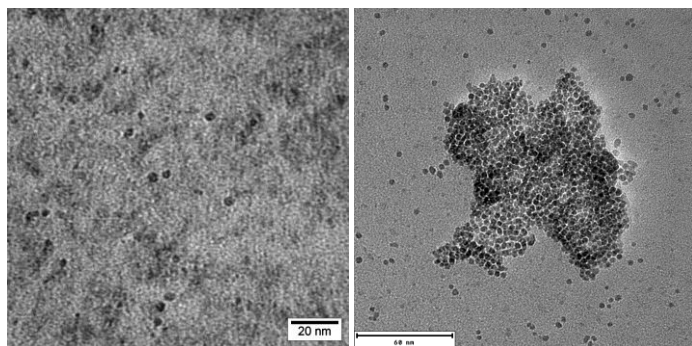


Fig. S54 TEM image of 1wt.-% Ru-NP in **4b** left: before catalysis; right: after 10 runs catalysis.

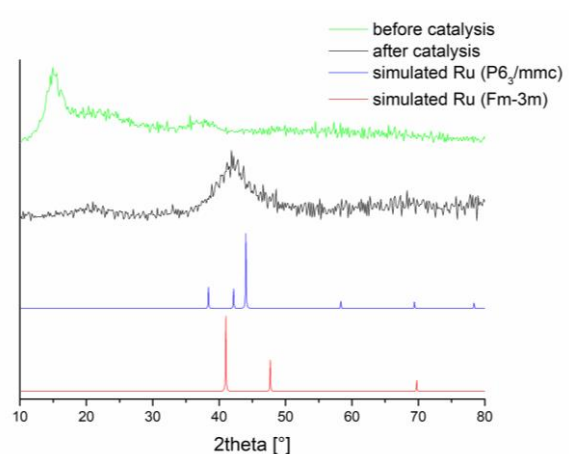


Fig. S55 PXRD of 1.0 wt.-% Ru-NPs in **4b**. Black curve: Ru-NPs before catalysis; green curve: very small amount of Ru-NPs after catalysis (the reflection at 15 ° originated from the Si sample holder); blue and red diffractogram: simulation of hcp-Ru ($P6_3/mmc$) from COD: 1932423 and of fcc Ru ($Fm\text{-}3m$) from COD: 1534914, respectively.

References

- 1 S. Ahrens, A. Peritz, T. Strassner, *Angew. Chem. Int. Ed.*, 2009, **48**, 7908 –7910.
- 2 M. Kaliner, A. Rupp, I. Krossing, T. Strassner, *Chem. Eur. J.*, 2016, **22**, 10044 – 10049.
- 3 F. Schroeter, S. Lerch, M. Kaliner, T. Strassner, *Org. Lett.*, 2018, **20**, 6215–6219.
- 4 C. Held, T. Reschke, S. Mohammad, A. Luza, G. Sadowski, *Chem. Eng. Res. Des.*, 2014, **92**, 2884–2897.
- 5 M. Bülow, X. Ji, C. Held, *Fluid Phase Equilib.*, 2019, submitted
- 6 K. Klauke, D. H. Zaitsau, M. Bülow, L. He, M. Kłopotowski, T.-O. Knedel, J. Barthel, C. Held, S. P. Verevkin, C. Janiak, *Dalton Trans.*, 2018, **47**, 5083–5097.
- 7 X. Ji, C. Held, G. Sadowski, *Fluid Phase Equilib.*, 2012, **335**, 64–73.
- 8 X. Ji, C. Held, G. Sadowski, *Fluid Phase Equilib.*, 2014, **363**, 59–65.
- 9 C. Held, L. F. Cameretti, G. Sadowski, *Fluid Phase Equilib.*, 2008, **270**, 87–96.
- 10 M. Antosik, M. Galka, S. K. Malanowski, *J. Chem. Eng. Data*, 2004, **49**, 11–17.
- 11 DIPPR table of Physical and Thermodynamic properties of pure compounds, AIChE, New York, 1998.
- 12 K. Ruzicka, V. J. Majer, *Phys. Chem. Ref. Data*, 1994, **23**, 1–27.
- 13 A. P. Umpierre, E. de Jesffls, J. Dupont, *ChemCatChem*, 2011, **3**, 1413–1418.
- 14 O. M. Wilson, M. R. Knecht, J. C. Garcia-Martinez, R. M. Crooks, *J. Am. Chem. Soc.*, 2006, **128**, 4510–4511.
- 15 A. Borodzinski, M. Bonarowska, *Langmuir*, 1997, **13**, 5613–5620.
- 16 H. Hosseini-Monfared, H. Meyer, C. Janiak, *J. Mol. Catal. A*, 2013, **372**, 72–78.
- 17 W. Zhang, H. Zhao, L. Wang, *J. Phys. Chem. B*, 2004, **108**, 2140–2147.
- 18 R. E. Benfield, *J. Chem. Soc. Faraday Trans.*, 1992, **88**, 1107–1110.